INVESTIGATION OF PHOTOELECTRON SPECTROSCOPY

FINAL REPORT

Contract NAS5-23054

Prepared for

National Aeronautics and Space Administration
Goddard Space Flight Center
Greenbelt, Maryland

DATE

February, 1973

Prepared by:

J. A. R. Samson
Principal Investigator

Behlen Laboratory of Physics
University of Nebraska
Lincoln, Nebraska

TABLE OF CONTENTS

INTRODUCTION

This is the final report of an "Investigation of Photoelectron Spectroscopy" supported under contract NAS5-23054.

During the period of this contract considerable attention was paid to the problem of obtaining true and meaningful branching ratios from the photoelectron spectra. That is, what relationship does the relative intensities of a photoelectron spectra have with the actual transition probabilities for transitions into the various electronic and vibrational levels of a molecule. Since this is the central problem in obtaining meaningful results considerable efforts were expended on this problem. The problem consists of understanding the transmission of an electron energy analyzer for electrons with different energies, understanding the effects of using partially polarized radiation from different vacuum monochromators, and in understanding the effects of the angular distribution of photoelectrons ejected from different orbitals.

An analysis of the degree of polarization of our monochromatic radiation and of the problem of varying angular distributions led to the construction of a cylindrical mirror electron energy analyzer set at the special angle of 54° 44' so that no discrimination would occur for electrons of different angular distributions. With the analyzer properly calibrated for transmission for electrons of different energies data were taken at several wavelengths and for several atmospheric gases. The results of this work are summarized in the following pages. Details of this work are to be found in the

following publications generated under this contract.

1. Branching Ratios in Photoelectron Spectroscopy, J. A. R. Samson and J. L. Gardner, J. Opt. Soc. Am. 62, 856 (1972).
2. Photoionization and Photoabsorption Cross Sections of CO_2 at 584 A, J. A. R. Samson, J. L. Gardner, and J. E. Mentall, J. Geophys. Res. 77, 5560 (1972).
3. Fluorescent Cross Sections and Yields of CO_2^+ from Threshold to 185 A, J. A. R. Samson and J. L. Gardner, J. Chem. Phys. (15 April 1973).
4. Fluorescence Excitation and Photoelectron Spectra of CO_2 Induced by Vacuum Ultraviolet Radiation Between 185 and 716A, J. A. R. Samson and J. L. Gardner, (Submitted J. Geophys. Res. Jan. 1973).

During the period of this contract the following papers were presented at the Meeting of the Optical Society of America, San Francisco, Oct. 17-20, 1972.

1. "304 Å Photoelectron Spectra of Atmospheric Molecules" J. L. Gardner and J. A. R. Samson.
2. "Absorption Cross Sections of Molecules between 100 and 600 Å," G. Haddad and J. A. R. Samson.

Further work performed under this contract will be presented at the Optical Society Meeting in Denver, March 13-16, 1973 as follows.

1. "Photoelectron spectra of nitric oxide between 950 and 1338Å" J. L. Gardner and J. A. R. Samson.
2. "Photoionization of Molecules between 20 and 100 eV" G. Haddad and J. A. R. Samson.

EXPERIMENTAL

The cylindrical mirror electron energy analyzer is shown in Fig. 1. The electrons formed in the ionizing region can only enter the analyzer provided they travel at an angle of 54° 44' with respect to the direction of the photon beam. Before entering the analyzer the electrons are retarded or accelerated to 3 volts. The analyzer voltage is set to allow only 3 volt electrons to pass through the exit slit and be counted by the Spiraltron. The advantage of this procedure is to provide a constant ΔE resolution no matter how energetic are the initial electrons. Without a retarding potential the analyzer's resolution $\Delta E/E$ is constant which means ΔE increases at the same rate as E. The present arrangement gave a ΔE = 40 mV for many of the measurements. A "best" ΔE of about 25 mV has been obtained.

The transmission of the analyzer was obtained by measuring the electron spectrum from argon. At the low pressures used in the analyzer's ion source the ratio of electron signal i_e to the incident flux I_o was proportional to the photoionization cross section σ_i, thus

$$\sigma_i = K \frac{i_e}{I_o}.$$

By measuring i_e and I_o and using the published values of σ_i it was possible to calculate K. If no discrimination against electrons of different energies exist then K will be constant as a function of electron energy. If discrimination exists K

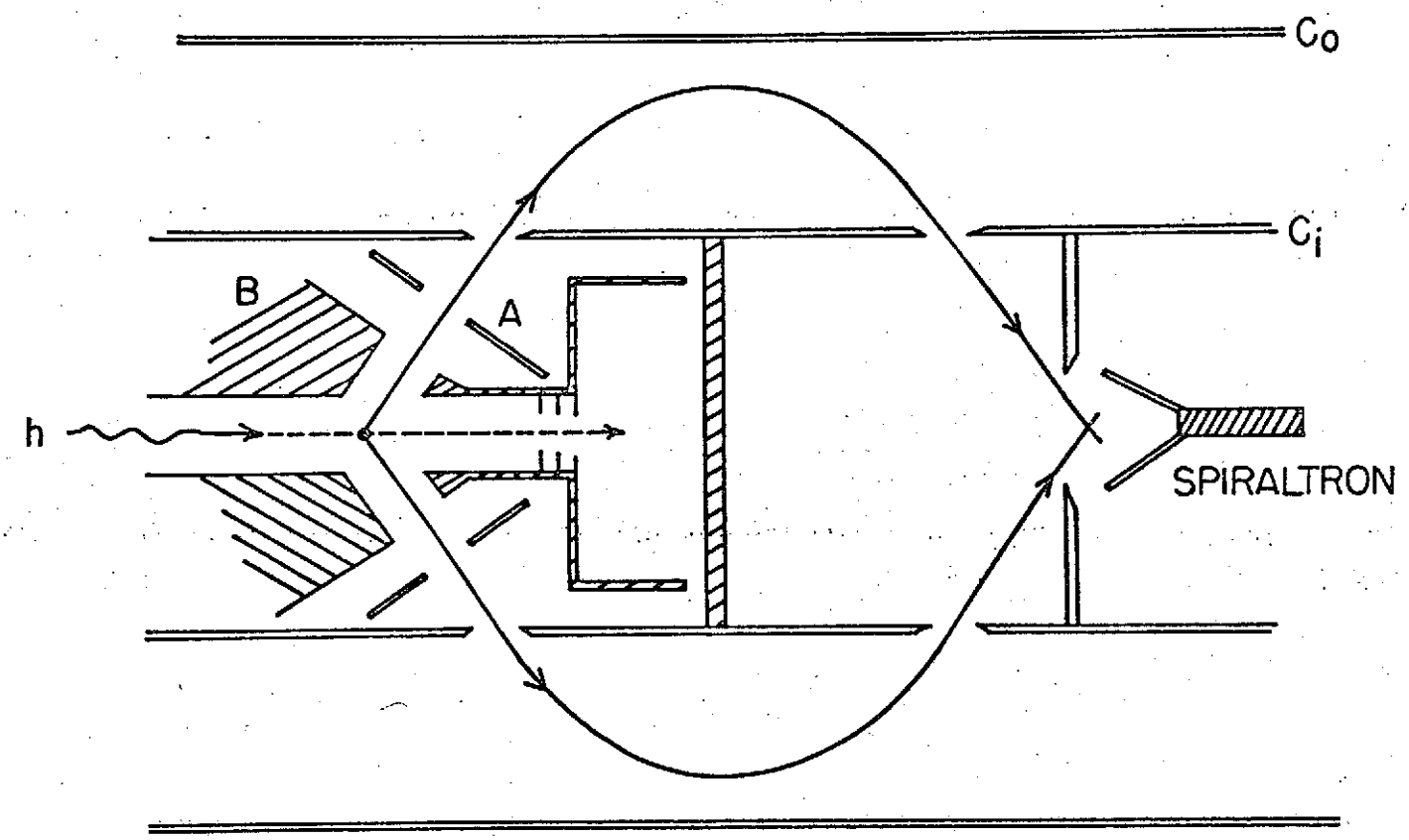

Fig. 1

will vary. However, K will represent the relative collection efficiency of electrons as a function of their energy. Figure 2 shows typical efficiency curves for the analyzer when no pre-retarding voltage is used and when fixed analyzing voltages of 3V and 1.5 V were used.

In all cases the collection efficiency was relatively constant between 4 and 11 eV. However, in order to see electrons efficiently between 0 and 4 eV it was necessary to use a retarding (or accelerating) voltage.

Thus, all data taken with electrons of energies between 0 and 4 eV had to have a correction factor to adjust their abundances for losses or gains in the analyzer.

Another serious problem encountered was the selective discrimination of electrons within a narrow energy band. This was only observed with a variation of pressure within the ion source and is caused by electrons having a very high scattering cross section at certain energies. An example is given for CO. Figure 3a shows how the electron scattering cross section varies with electron energy. Between 1 and 2 eV the cross section varies by a factor of two. The branching ratios of the X, A, and B states of CO are shown in Fig. 3b as a function of pressure. The branching ratio of the X-state is defined as the abundance found in the X-state divided by the sum of the abundances found in the X + A + B states, etc. It is obvious that the effects of higher pressure produce false results and one must be careful to check for pressure effects.

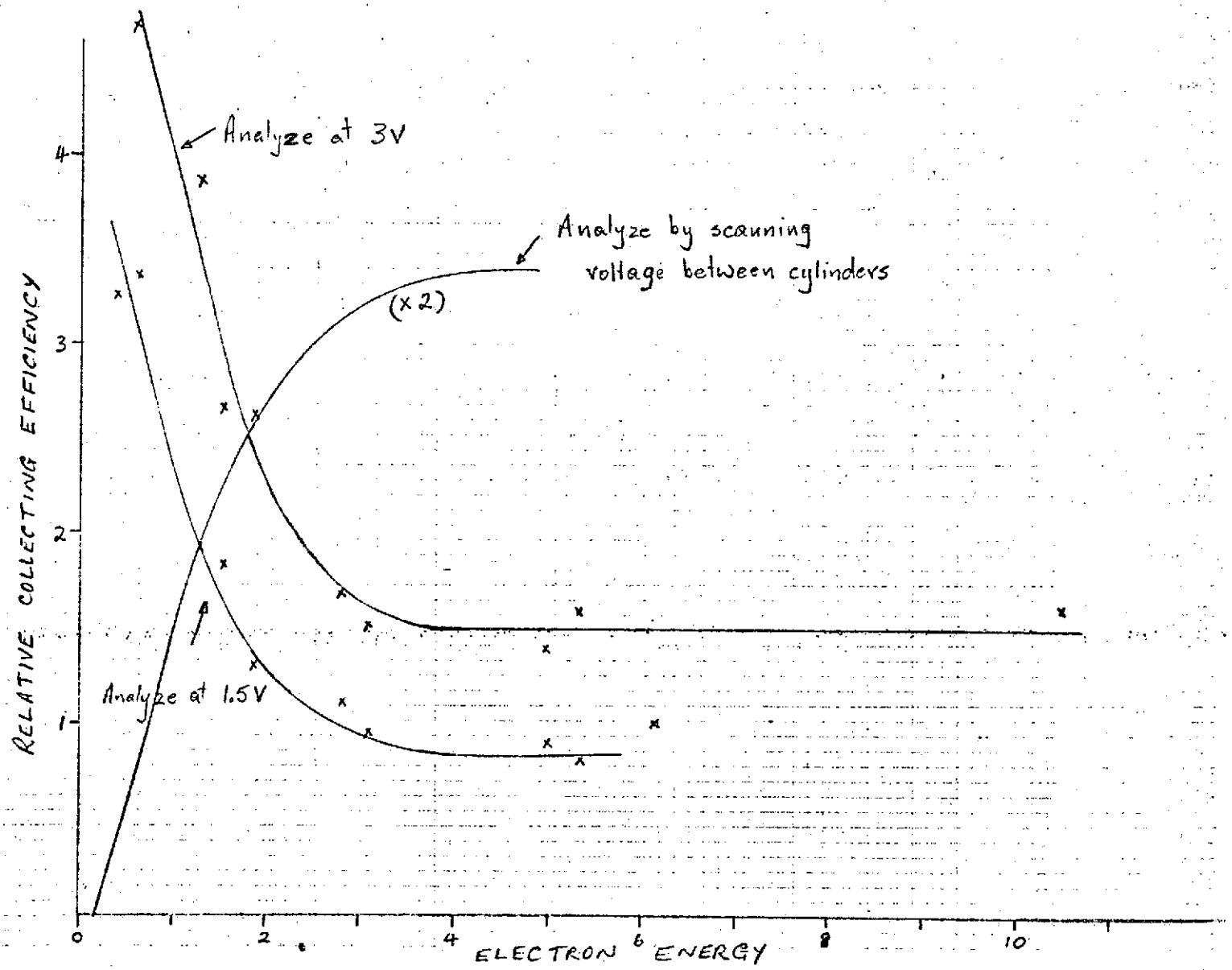
Analyze at 3V
Analyze by scanning voltage between cylinders
(x 2)
Analyze at 1.5V
RELATIVE COLLECTING EFFICIENCY
ELECTRON ENERGY
0
2
4
6
8
10
1
2
3
4

Fig. 2

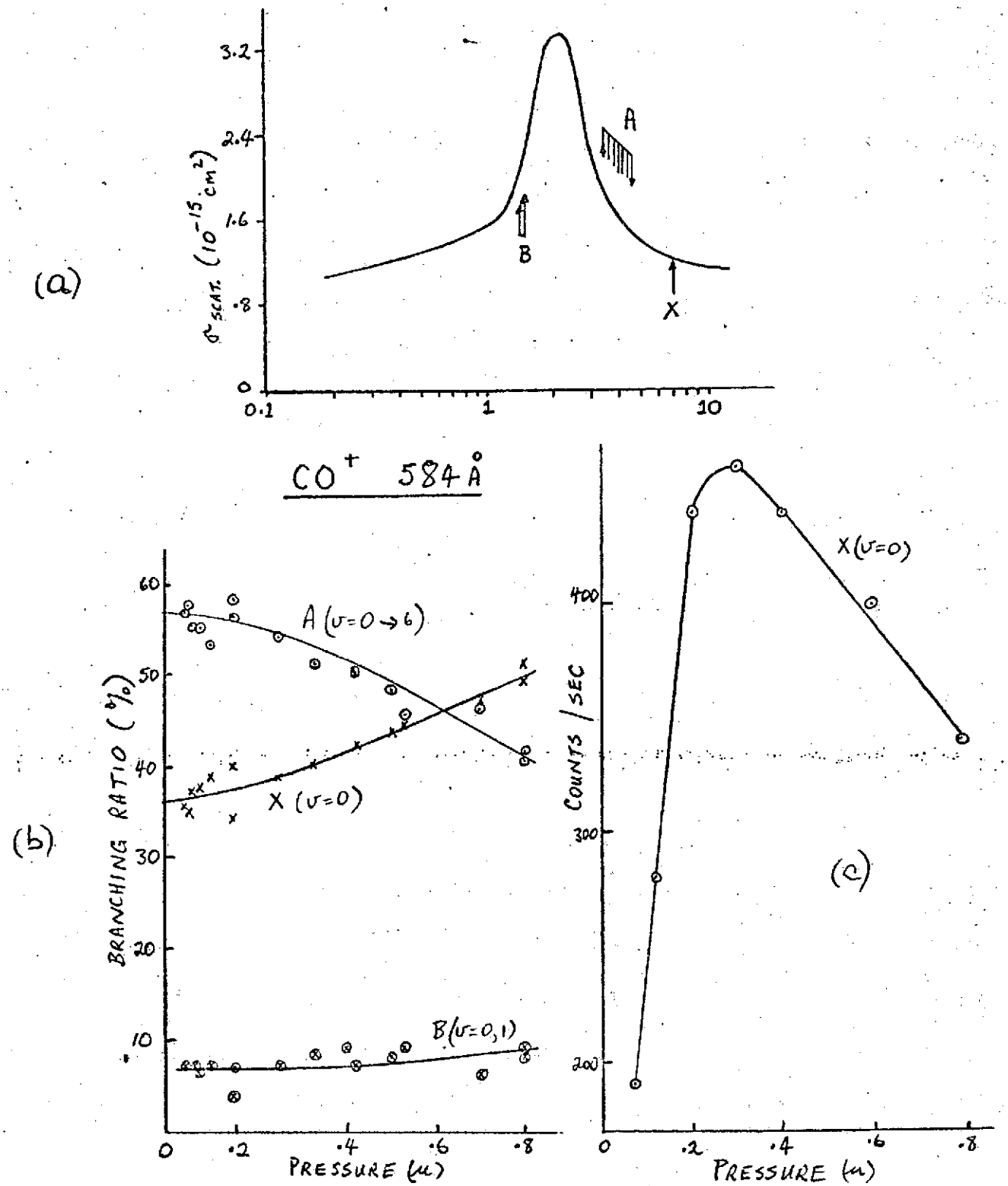
(a)
3.2
2.4
1.6
.8
0
$\sigma_{SCAT.}$ (10^{-15} cm^2)
0.1
1
10
A
B
X
CO^+ 584 Å
(b)
60
50
40
30
20
10
BRANCHING RATIO (%)
A (v=0→6)
X (v=0)
B (v=0,1)
0
.2
.4
.6
.8
PRESSURE (μ)
(c)
400
300
200
COUNTS / SEC
X (v=0)
0
.2
.4
.6
.8
PRESSURE (μ)

Fig. 3

To check the validity that an analyzer based on the angle of 54°44' will indeed provide true branching ratios independent of the angular distribution of the photoelectron the $^2P_{3/2}$ to $^2P_{1/2}$ ratio in the rare gases was checked (Figs. 4 and 5). The ratio has been measured previously by the author using a spherical grid retarding potential analyzer. This analyzer was sensitive to both the angular distribution and the degree of polarization of the radiation. Although the degree of polarization was known the angular distribution of the two groups of electrons was not known. Recently, unpublished theoretical data by D. Dill of the University of Chicago became available which provided the missing values of the angular distribution. With this new set of data the $^2P_{3/2}$ to $^2P_{1/2}$ ratio for the retarding potential analyzer was corrected and compared with the present data from the cylindrical mirror analyzer. The results are shown in Fig. 6 The corrected results are in good agreement with the present results. It can be seen that when there is information about the angular distribution corrections to the data can be made using paper No. 1 (J.O.S.A. 62, 856(1972)). However, in most cases there is no angular distribution data and it is necessary to use an analyzer such as the present one based on the 54°44' angle.

RESULTS

The results are presented primarily as photoelectron spectra of various atmospheric gases at various wavelengths. In some cases detailed analysis of the intensities of the vibrational levels have been completed and compared with

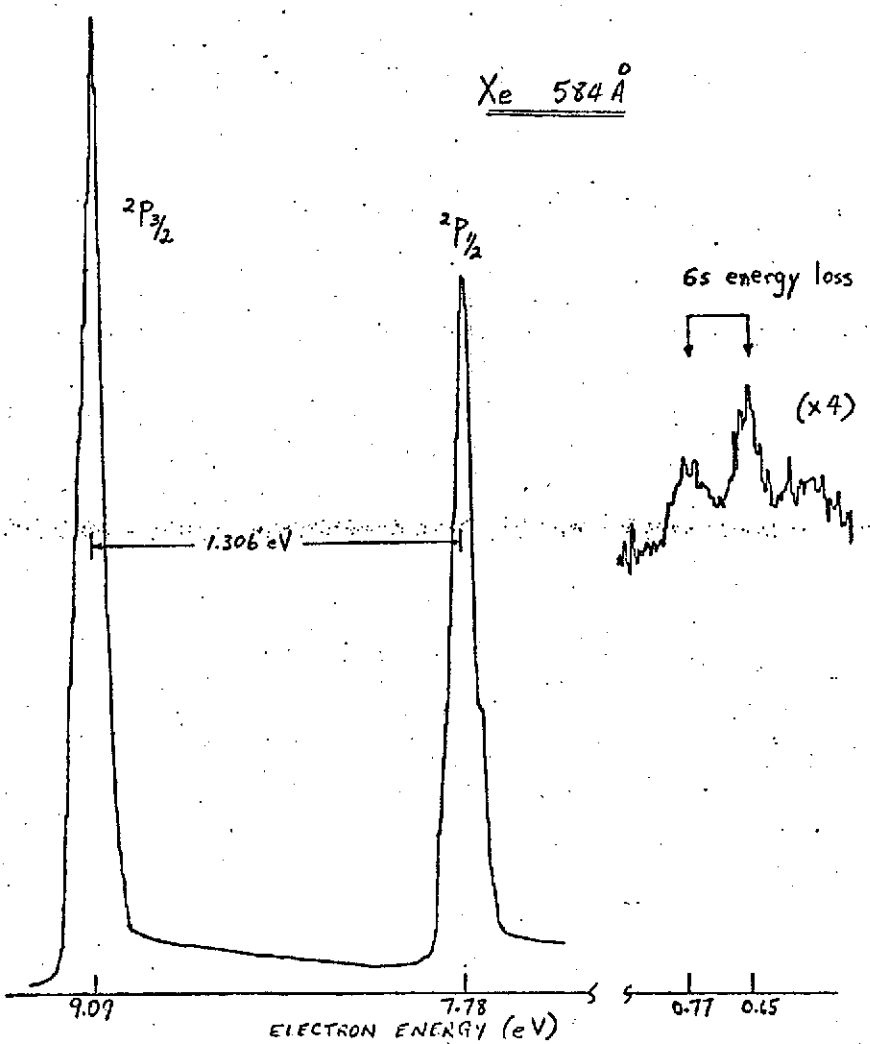
Xe 584 Å
$^2P_{3/2}$
$^2P_{1/2}$
1.306 eV
6s energy loss
(x4)
9.09
7.78
0.77
0.45
ELECTRON ENERGY (eV)

Fig. 4

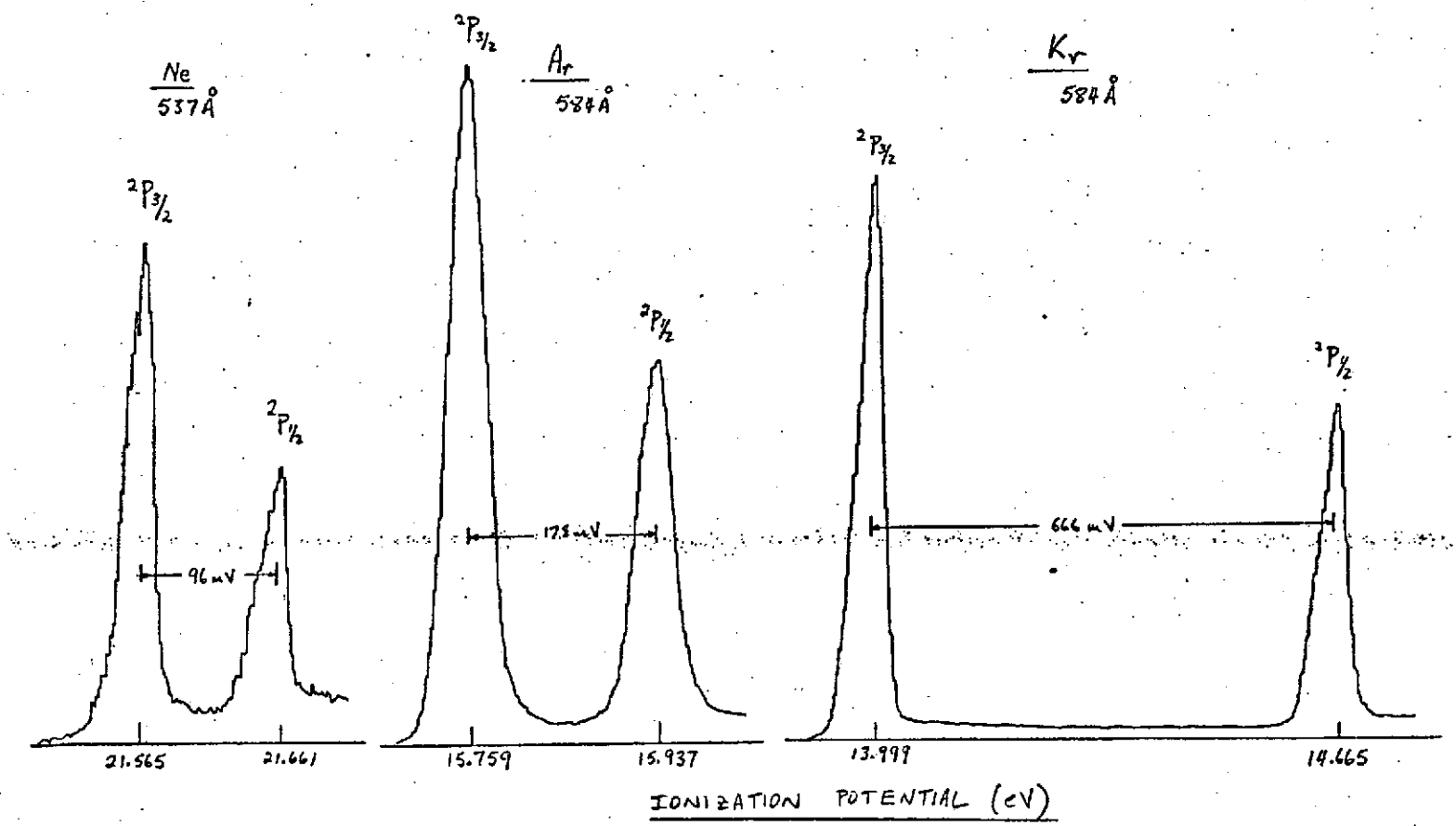
Ne
537Å
$^2P_{3/2}$
$^2P_{1/2}$
96 mV
21.565
21.661
$^2P_{3/2}$
Ar
584Å
$^2P_{1/2}$
178 mV
15.759
15.937
Kr
584Å
$^2P_{3/2}$
$^2P_{1/2}$
666 mV
13.999
14.665
IONIZATION POTENTIAL (eV)

Fig. 5

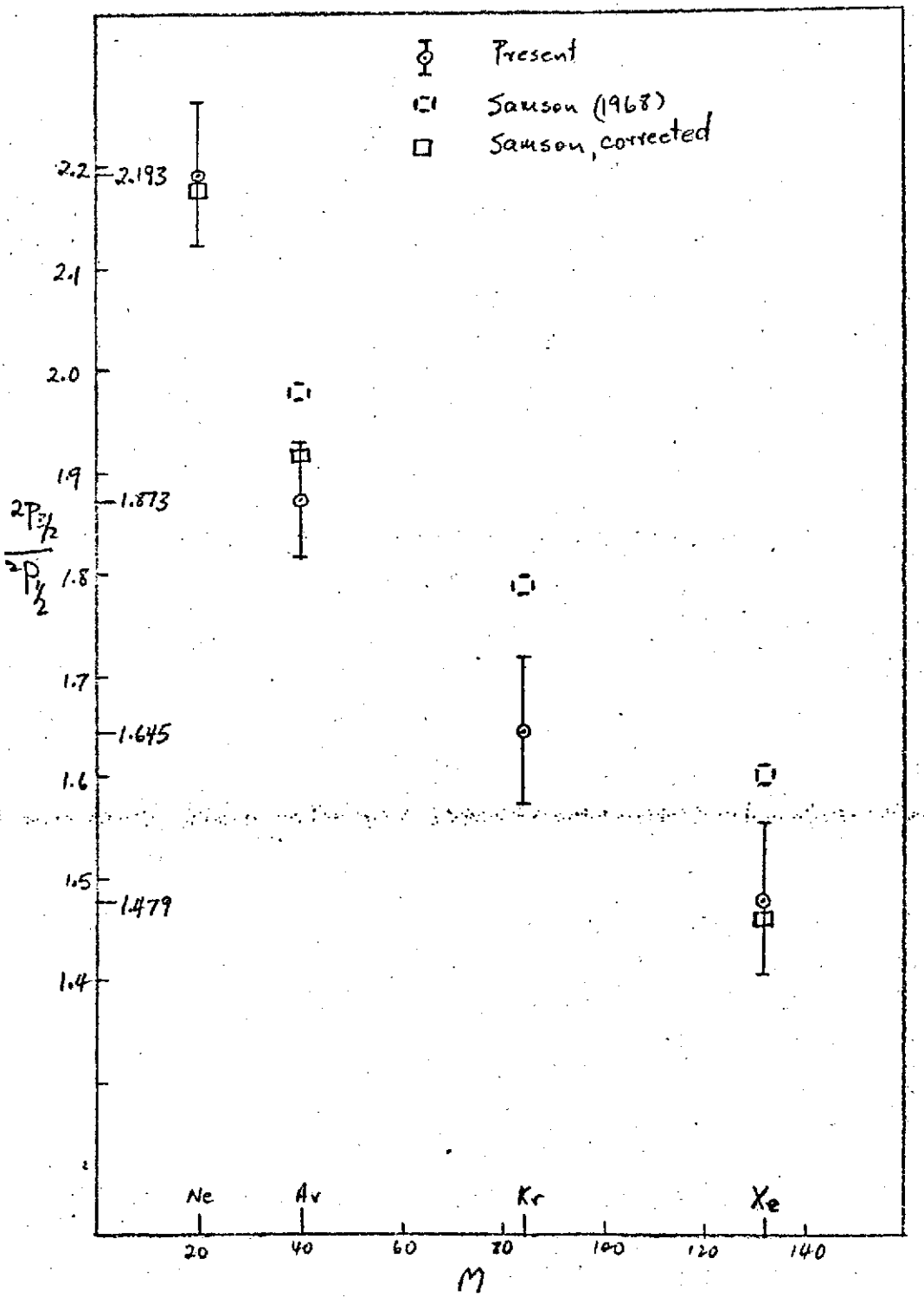
Present
Samson (1968)
Samson, corrected
2.2
2.193
2.1
2.0
1.9
1.873
1.8
1.7
1.645
1.6
1.5
1.479
1.4
$\frac{^2P_{3/2}}{^2P_{1/2}}$
Ne
Ar
Kr
Xe
20
40
60
80
100
120
140
M

Fig. 6

theoretical Franck-Condon factors. Analyses of many of the spectra are continuing and will appear in the scientific journals.

Hydrogen H_2:

The photoelectron (PE) spectra of hydrogen taken at 584Å is shown in Fig. 7. Eleven vibrational levels can be identified. The intensities of each of the vibrational bands has been corrected for instrumental error. The results are compared with the theoretical Franck-Condon factors in Fig. 8. Overall agreement is obtained. However, in detail many theoretical points lie outside of the expected experimental error bars.

Deuterium D_2:

Figure 9 shows the P.E. Spectra of deuterium with 17 vibrational levels resolved. The corrected relative intensities of these bands are shown in Fig. 10 and compared with theoretical calculations. Again, overall agreement is very good.

Oxygen O_2:

The PE spectra of oxygen has been measured at 584, 537, and 304Å. These spectra are shown in Figs. 11, 12, and 13, respectively. The branching ratios for the population of the various electronic states are tabulated in Table 1. The results at 304Å present new data. Transitions accounting for approximately 38% of the ionic abundance go into the removal of $\sigma 2s$ electrons leaving the ions in the excited $^2\Sigma^-$ and $^4\Sigma^-$ states. These new states have thresholds of about 38.5 and

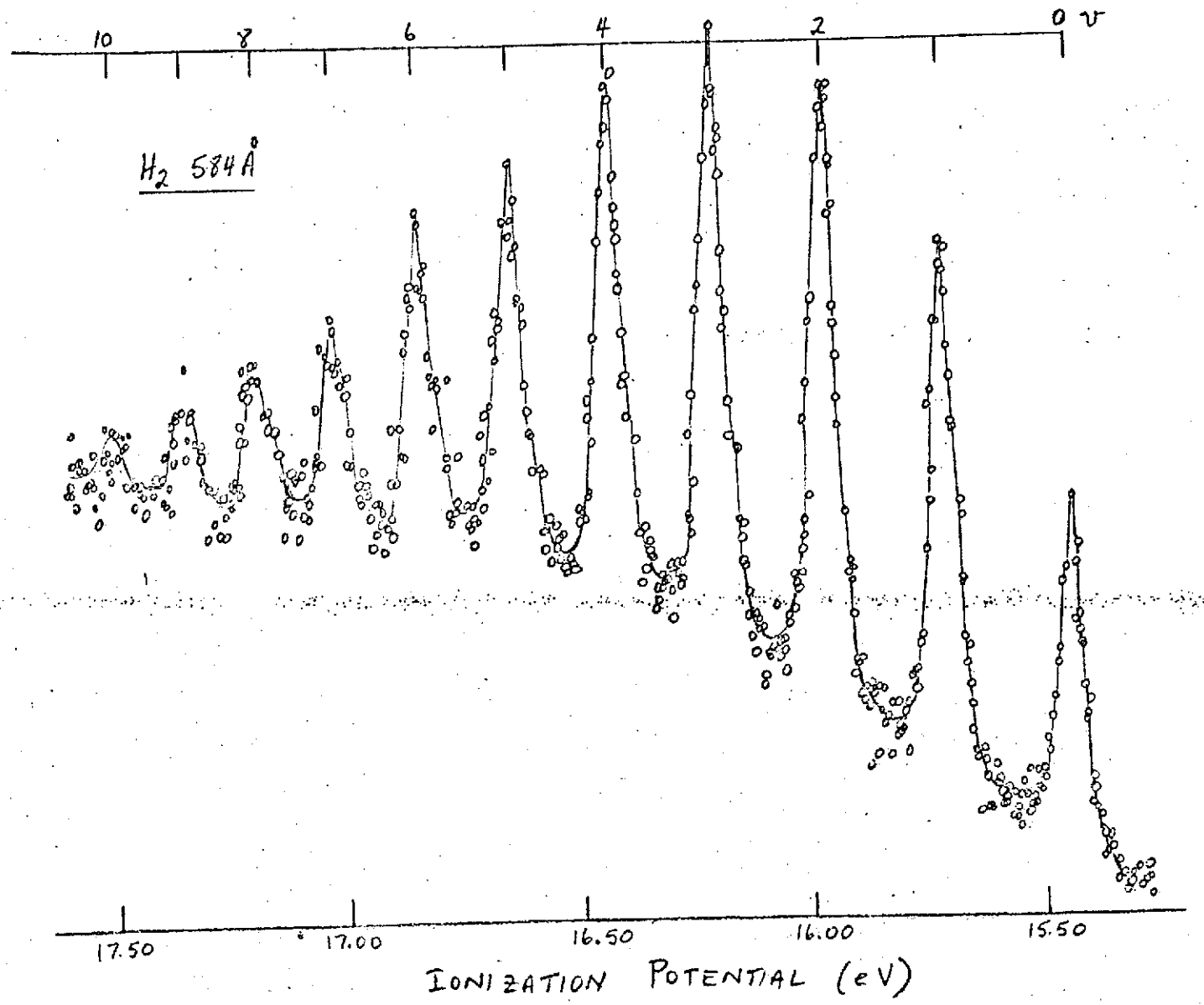
10
8
6
4
2
0 v
H2 584Å
17.50
17.00
16.50
16.00
15.50
IONIZATION POTENTIAL (eV)

Fig. 7

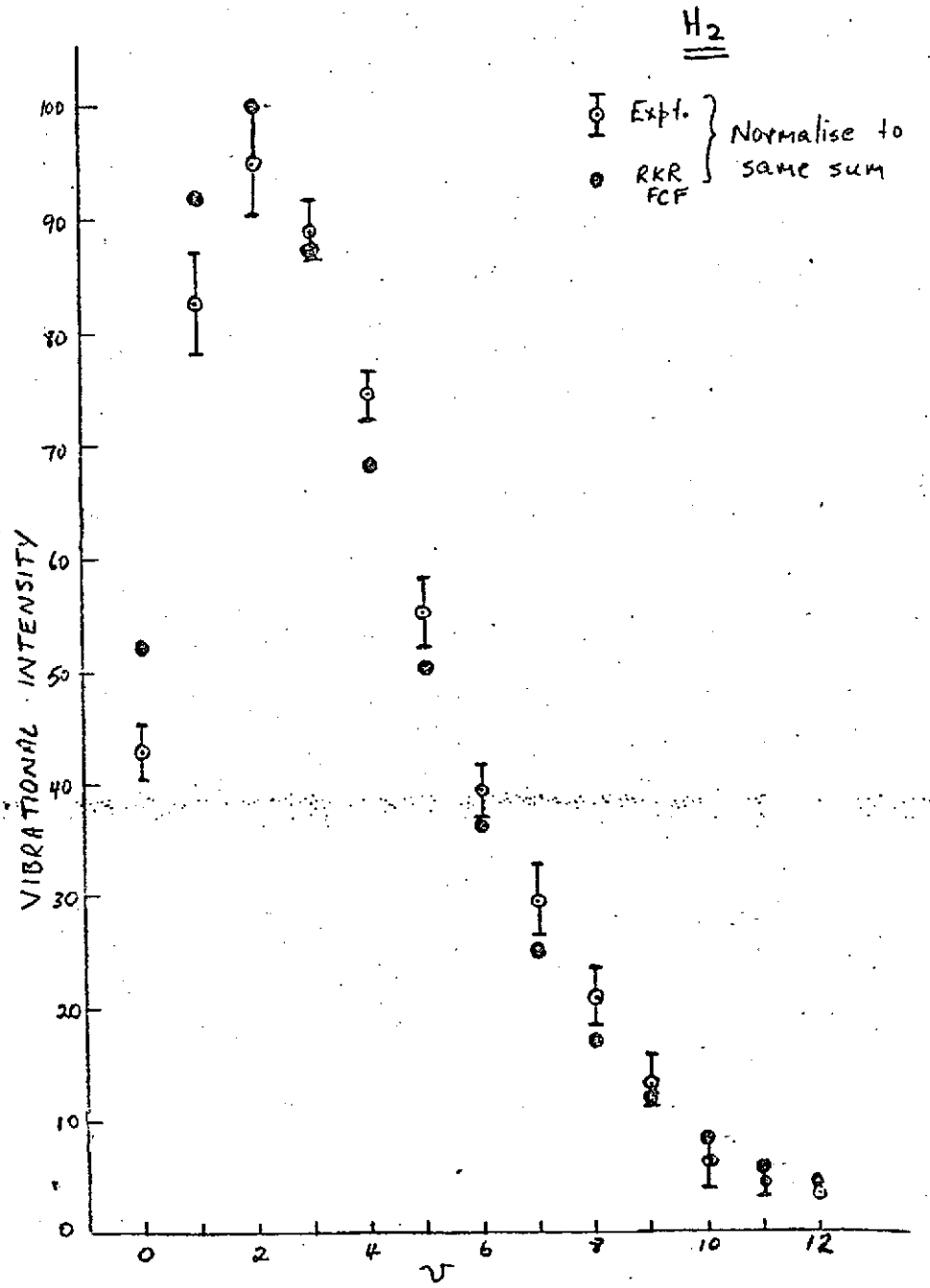
H_2
Expt.
RKR FCF
Normalise to same sum
VIBRATIONAL INTENSITY
100
90
80
70
60
50
40
30
20
10
0
0
2
4
6
8
10
12
v

Fig. 8

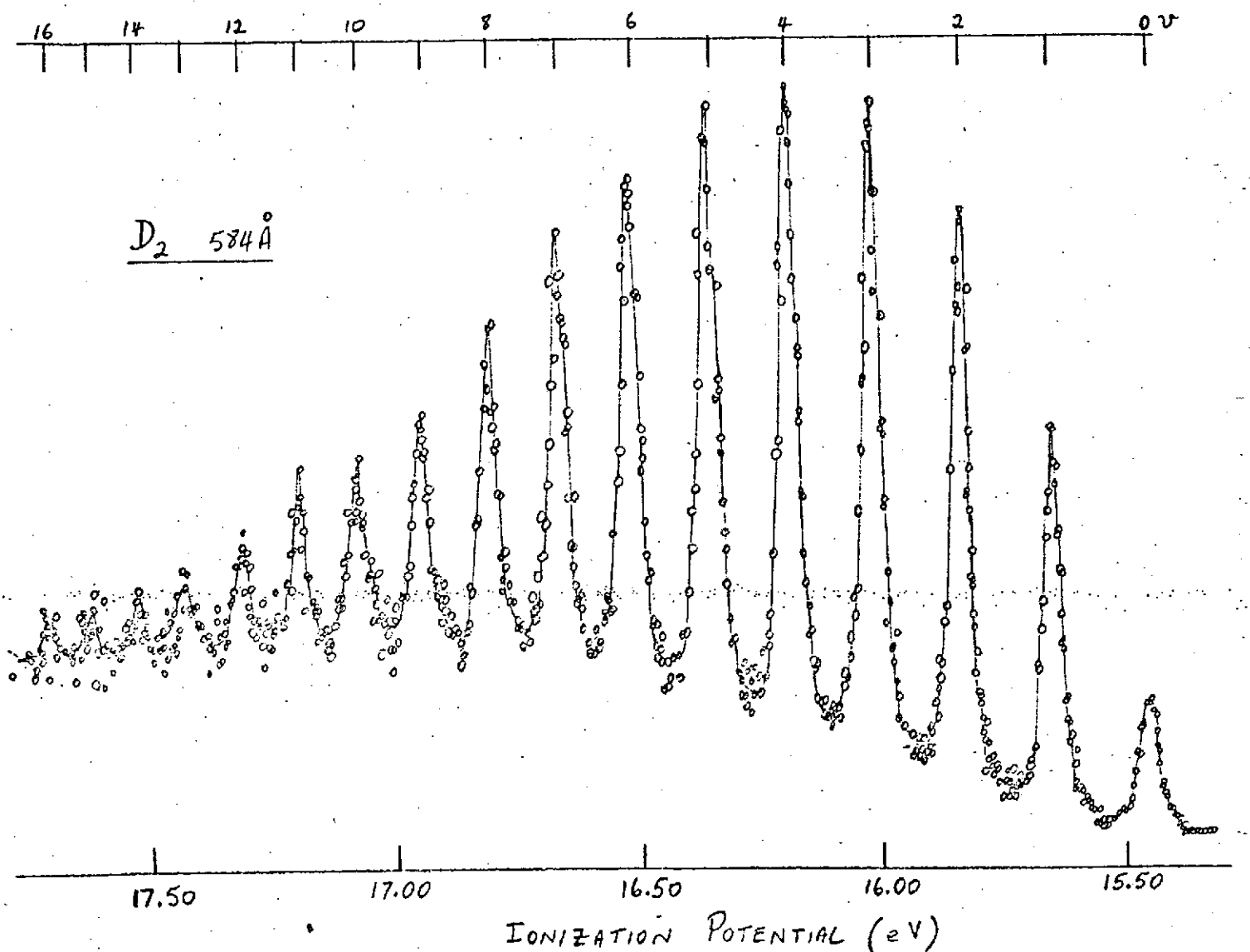
16
14
12
10
8
6
4
2
0 V
D2 584Å
17.50
17.00
16.50
16.00
15.50
IONIZATION POTENTIAL (eV)

Fig. 9

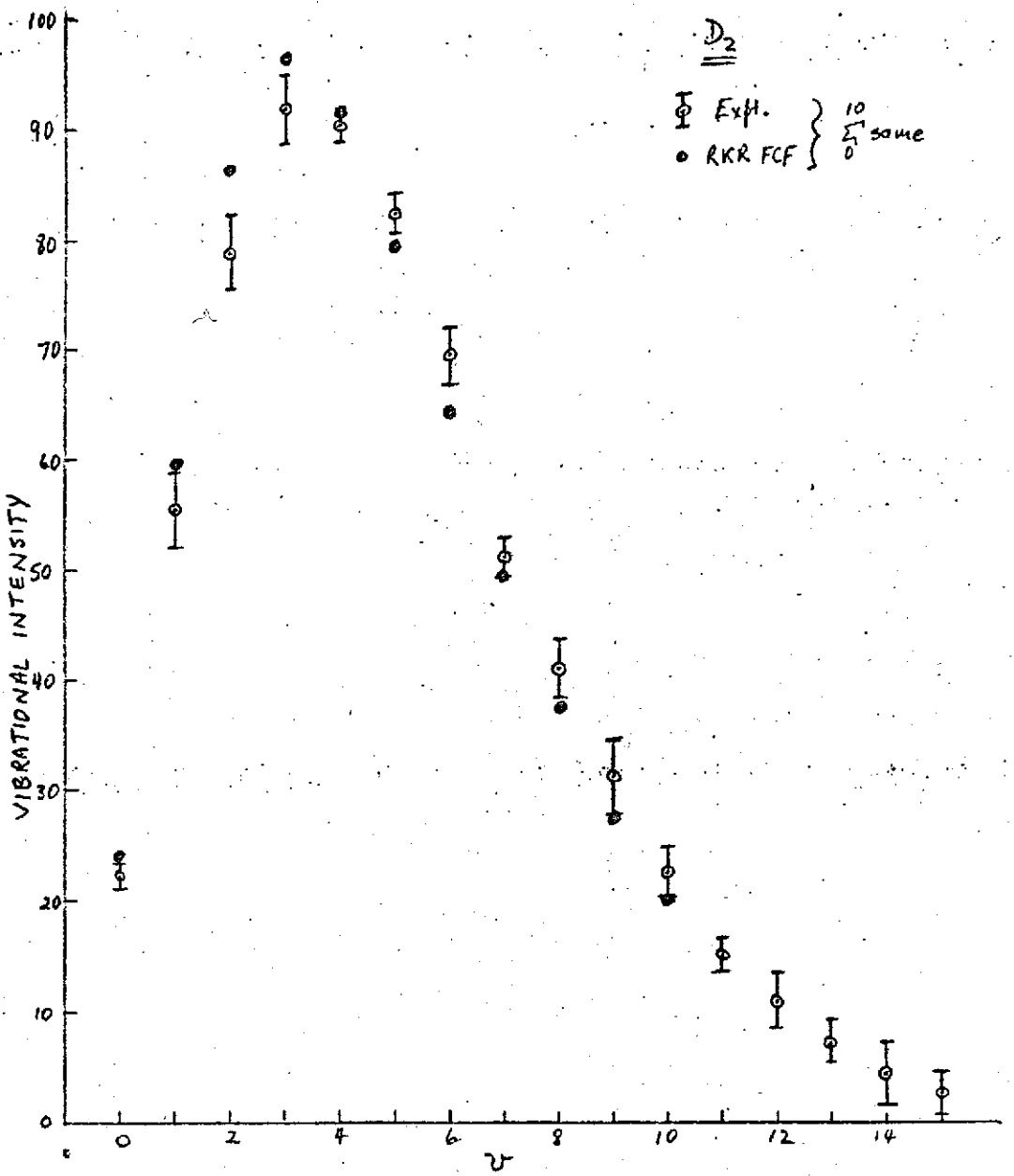
D_2
Exp't.
RKR FCF
$\sum_0^{10}$ some
VIBRATIONAL INTENSITY
100
90
80
70
60
50
40
30
20
10
0
0
2
4
6
8
10
12
14
v

Fig. 10

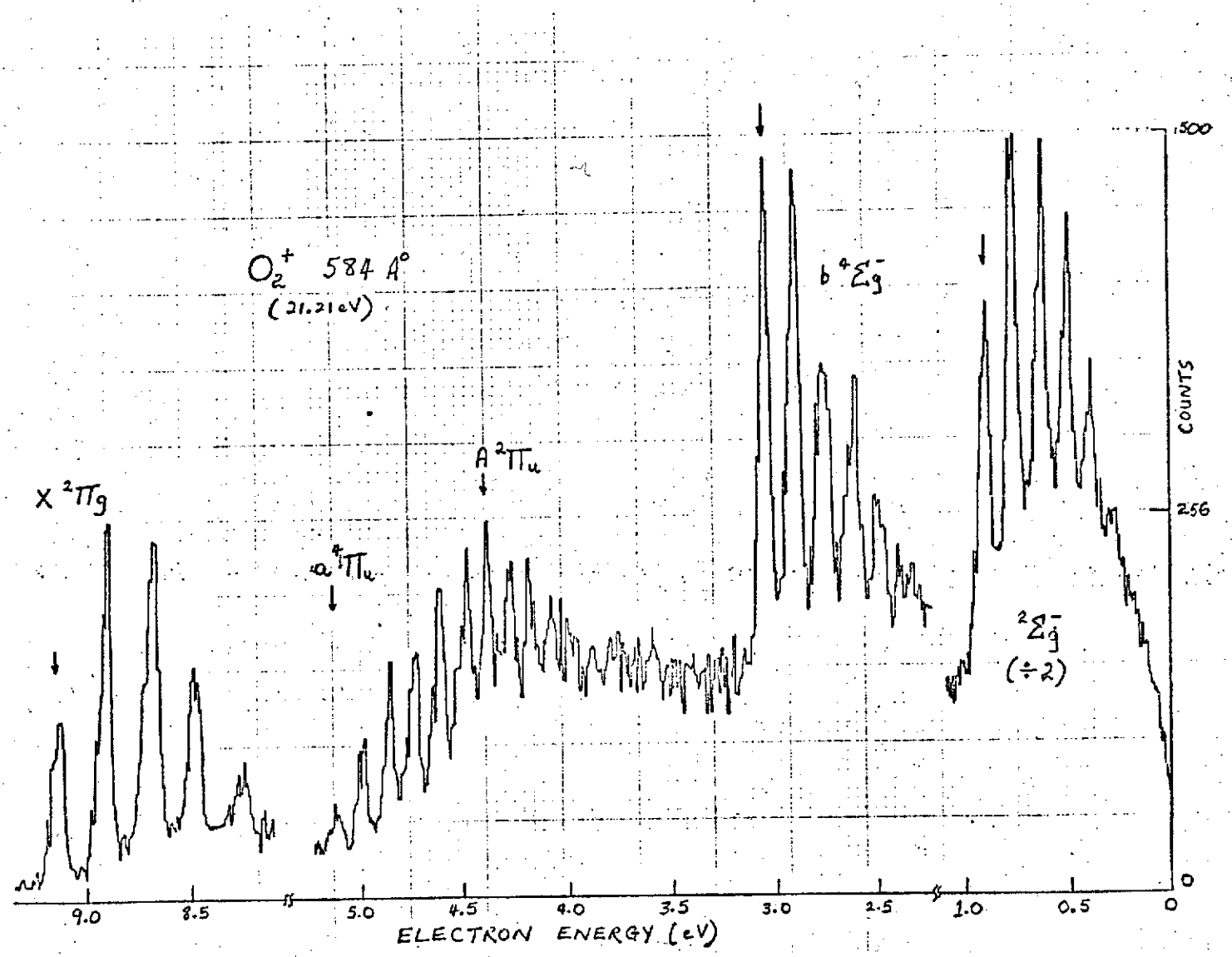
O_2^+ 584 A°
(21.21 eV)
$X\ ^2\Pi_g$
$a\ ^4\Pi_u$
$A\ ^2\Pi_u$
$b\ ^4\Sigma_g^-$
$^2\Sigma_g^-$
(÷2)
1500
256
0
COUNTS
9.0
8.5
5.0
4.5
4.0
3.5
3.0
2.5
1.0
0.5
0
ELECTRON ENERGY (eV)

Fig. 11

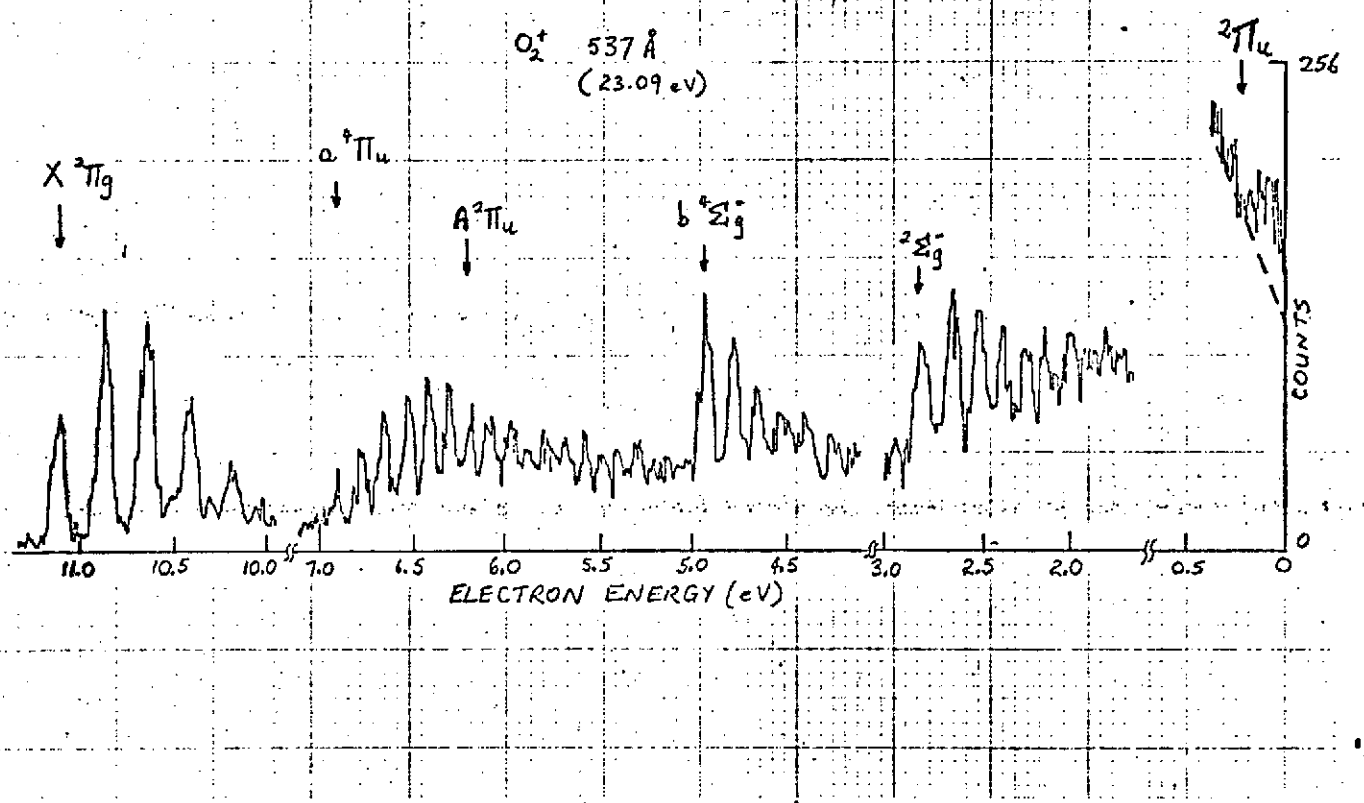
O_2^+ 537 Å
(23.09 eV)
$X\ ^2\Pi_g$
$a\ ^4\Pi_u$
$A\ ^2\Pi_u$
$b\ ^4\Sigma_g^-$
$^2\Sigma_g^-$
$^2\Pi_u$
256
COUNTS
0
11.0
10.5
10.0
7.0
6.5
6.0
5.5
5.0
4.5
3.0
2.5
2.0
0.5
0
ELECTRON ENERGY (eV)

Fig. 12

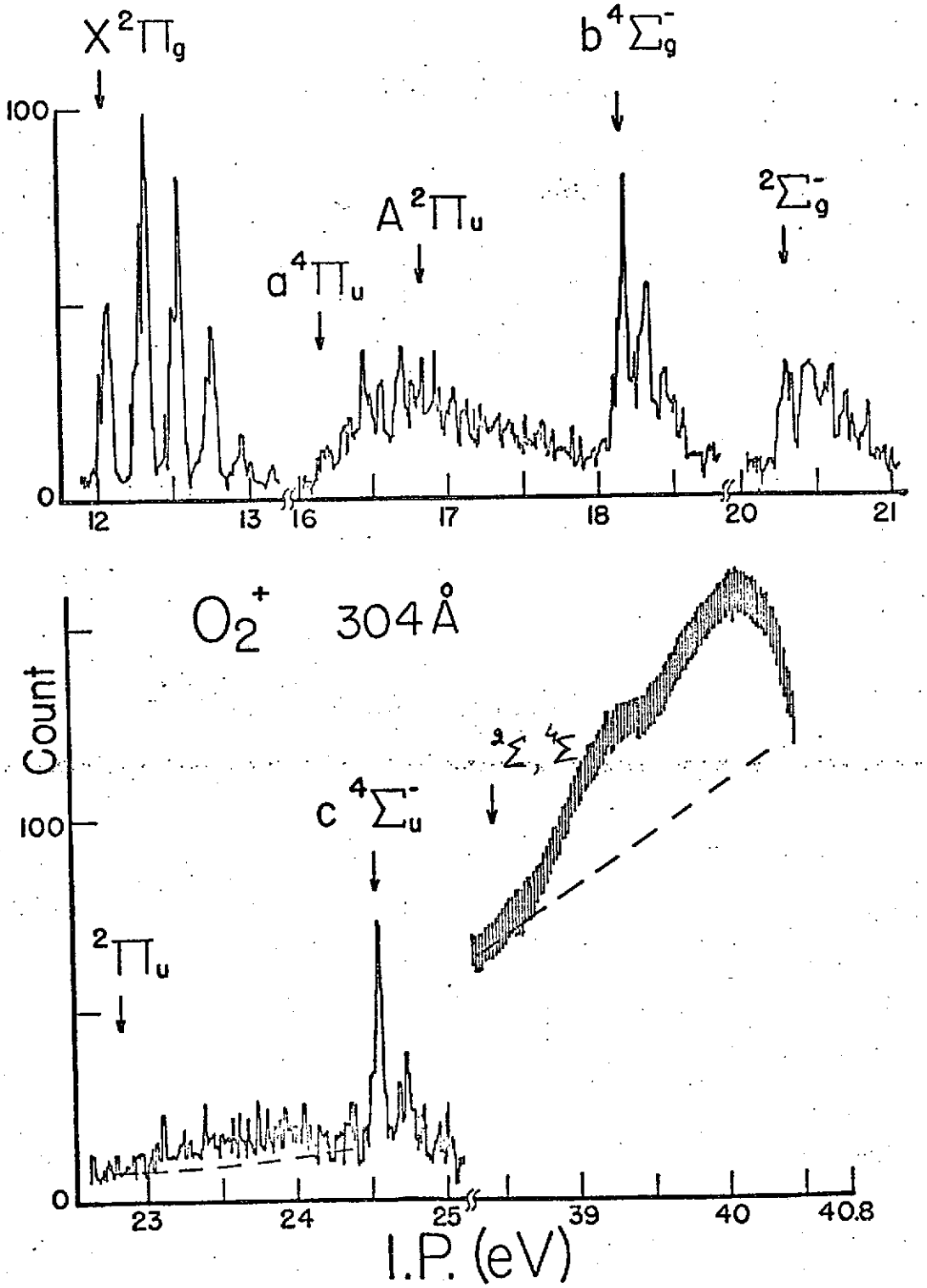
X ²Πg
b ⁴Σg⁻
100
A ²Πu
a ⁴Πu
²Σg⁻
0
12
13
16
17
18
20
21
O2⁺ 304 Å
Count
²Σ, ⁴Σ
c ⁴Σu⁻
100
²Πu
0
23
24
25
39
40
40.8
I.P. (eV)

Fig. 13

Table 1. Branching Ratios for O_2^+

O_2^+ State	Branching ratios (%) 584Å	537Å	304Å
X $^2\Pi_g$	22.9	32.1	16.5
a $^4\Pi_u$ + A $^2\Pi_u$	33.9	33.9	18.2
b $^4\Sigma_g^-$	27.0	14.4	9.2
$^2\Sigma_g^-$	16.3	18.0	6.9
$^2\Pi_u$	-	1.5	5.4
c $^4\Sigma_u^-$	-	-	5.4
$^2\Sigma$, $^4\Sigma$	-	-	38.2

39.5 eV. Thus, of the photoelectrons produced by 304Å in O_2 about 38% of them have energies less than 3 eV. Moreover, from Fig. 13 the structure of the new Σ-states can be seen to be continuous implying a dissociative ionization process possibly producing energetic atomic fragments (≈ 5-10 eV).

Nitrogen N_2

The 584Å PE spectra of nitrogen is shown in Fig. 14. An analysis of the vibrational distribution within each electronic state is given in Fig. 15. To study the vibrational levels of the B state a detailed study was made at various gas pressures within the analyzer's ion source. The results at two pressures 0.03 μ and 0.6 μ are shown in Fig. 16. The true v=0 and v=1 vibrational levels are seen in both cases. However, at the higher pressures new peaks appear. These peaks have been observed by Price as well and are attributed to an energy loss process. The B state (v=0) produces electrons of 2.47 eV energy. These electrons collide with neutral N_2 producing N_2^- in specific vibrational levels. These are unstable states which quickly auto-detach and eject the electron. The N_2^- state then relaxes into the appropriate vibrational level of the neutral N_2 molecule according to the Franck-Condon principle. Figure 17 illustrates the mechanism as explained by Price. This phenomena emphasizes the care that is necessary in obtaining true PE spectra.

In Fig. 18 the PE spectra of N_2 is shown taken with the 304Å line. New states are observed at 28.2, 36.5, and 38.7 eV. The continuum nature of these peaks suggests transitions into the repulsive region of the potential energy curves. Thus, dissociation processes appear to be strong at 304Å. Table 2 lists the electronic branching ratios for 584, 537, and 304Å.

Nitric Oxide NO:

The P.E. Spectrum of NO has been measured at many wave-

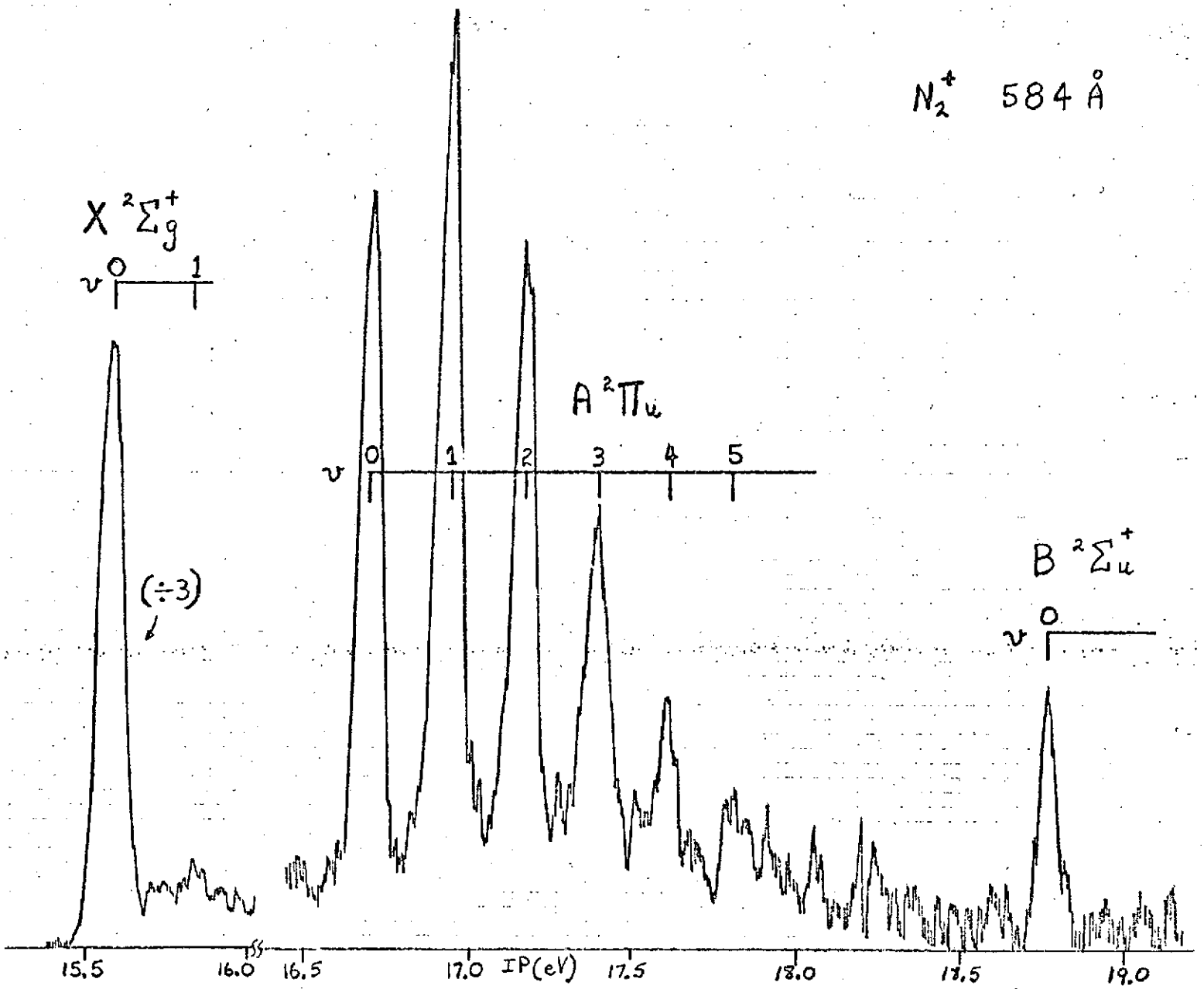
N_2^+ 584 Å
$X\ ^2\Sigma_g^+$
v 0 1
(÷3)
$A\ ^2\Pi_u$
v 0 1 2 3 4 5
$B\ ^2\Sigma_u^+$
v 0
15.5
16.0
16.5
17.0 IP(eV)
17.5
18.0
18.5
19.0

Fig. 14

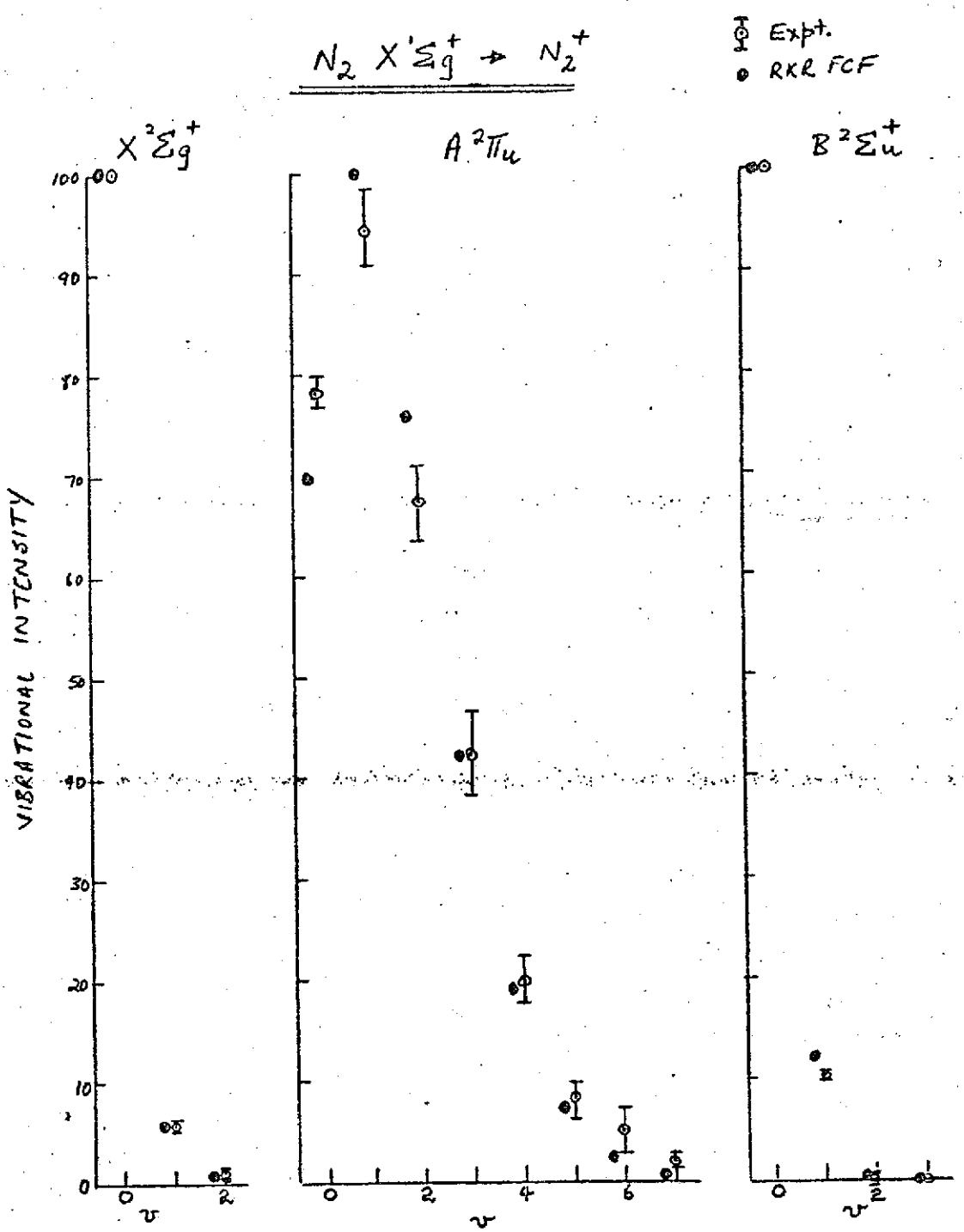
N_2 $X\,^1\Sigma_g^+ \rightarrow N_2^+$
Expt.
RKR FCF
$X\,^2\Sigma_g^+$
$A\,^2\Pi_u$
$B\,^2\Sigma_u^+$
VIBRATIONAL INTENSITY
100
90
80
70
60
50
40
30
20
10
0
v
0
2
4
6
v
0
v

Fig. 15

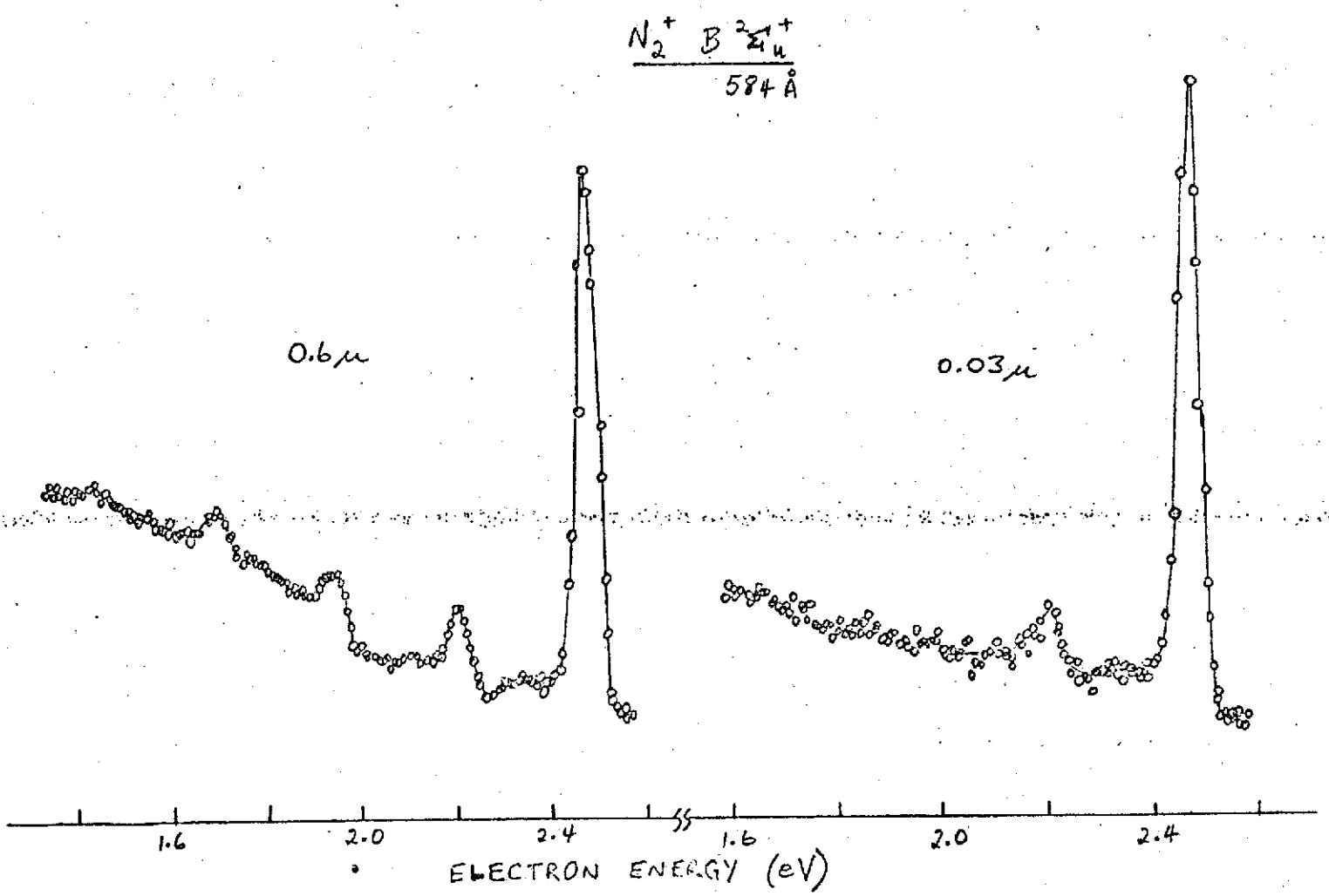

Fig. 16

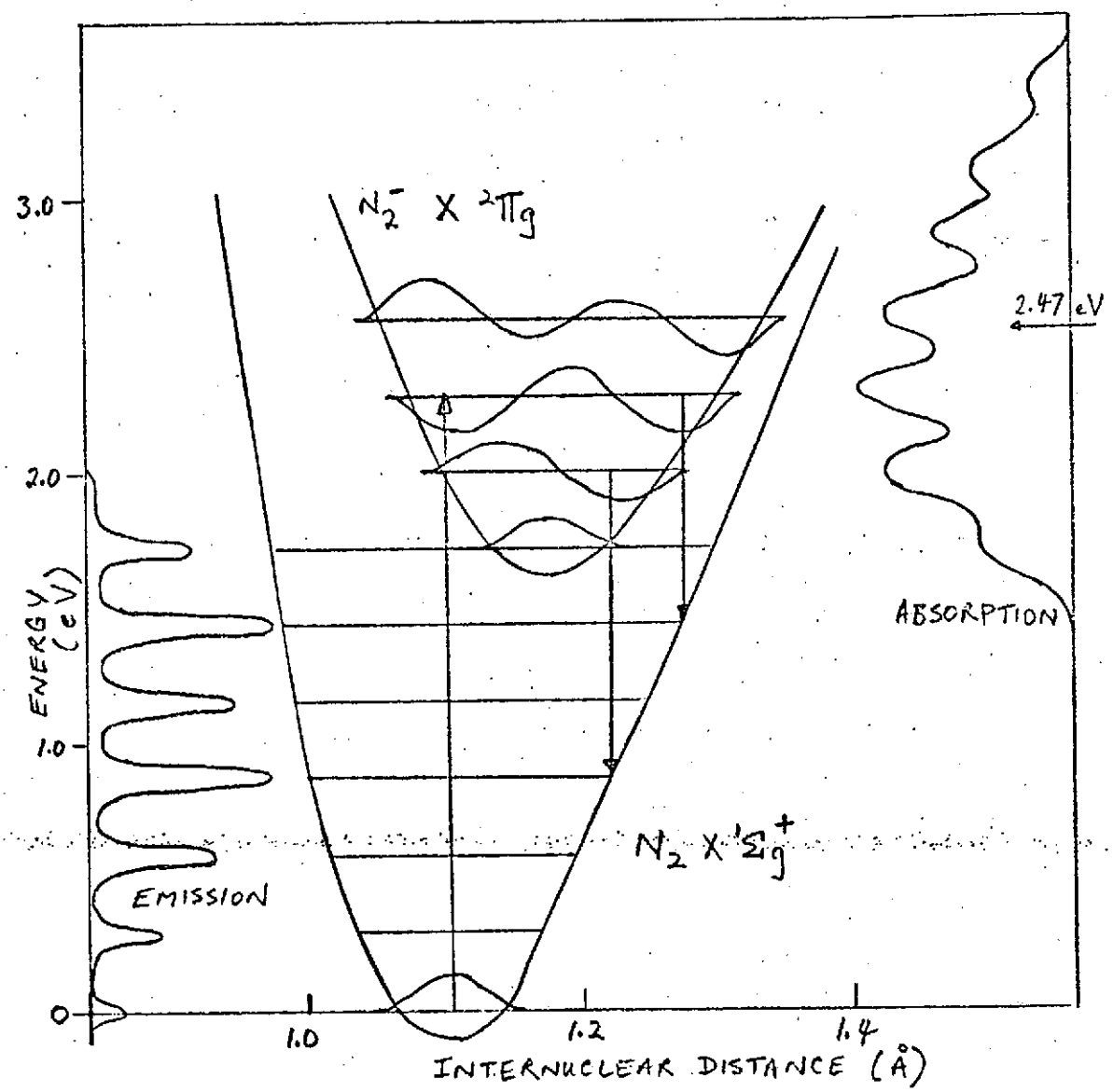
3.0
2.0
1.0
0
ENERGY (eV)
N_2^- X $^2\Pi_g$
N_2 X $^1\Sigma_g^+$
EMISSION
ABSORPTION
2.47 eV
1.0
1.2
1.4
INTERNUCLEAR DISTANCE (Å)

Fig. 17

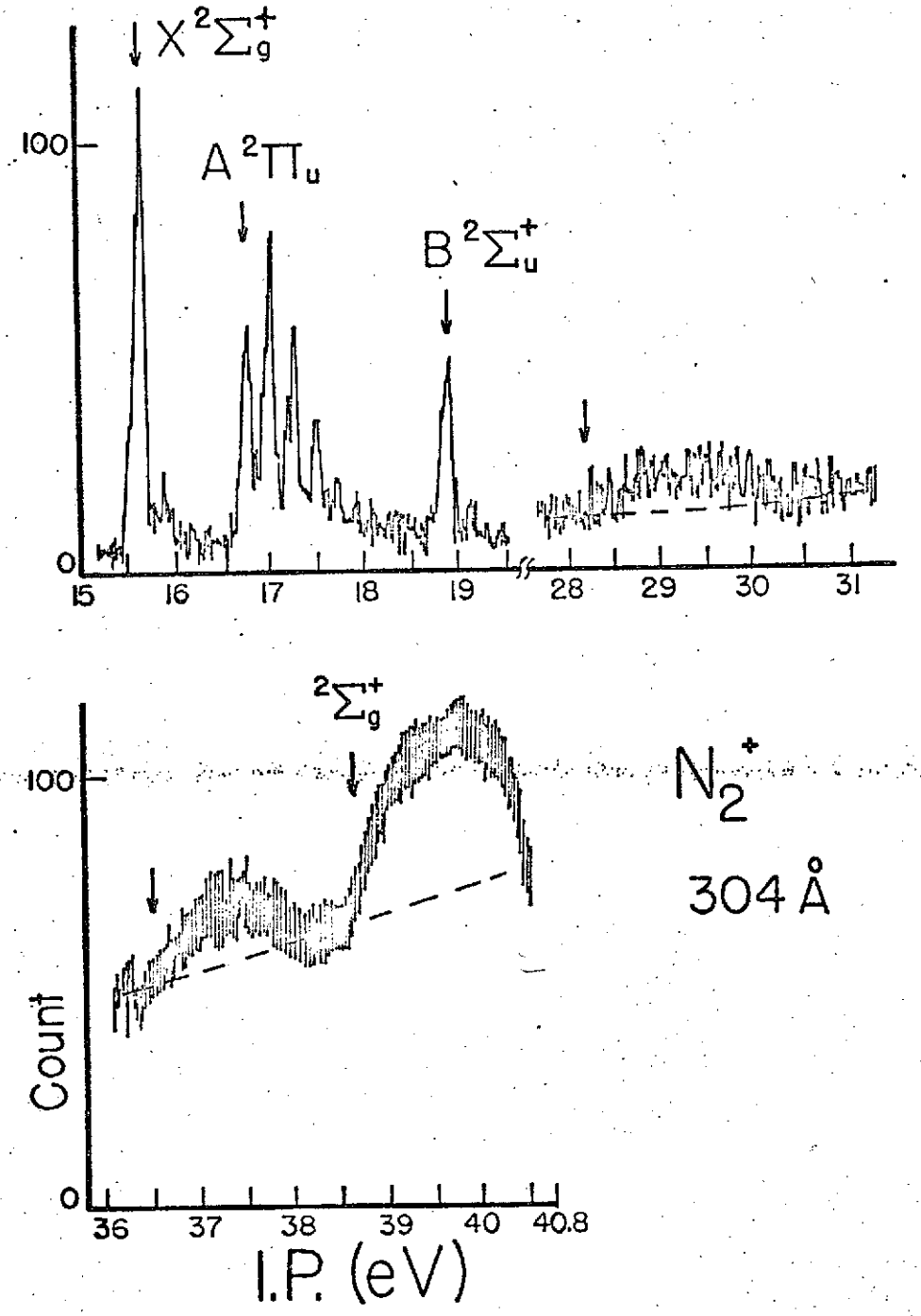
X $^2\Sigma_g^+$
A $^2\Pi_u$
B $^2\Sigma_u^+$
100
0
15
16
17
18
19
28
29
30
31
$^2\Sigma_g^+$
100
0
Count
36
37
38
39
40
40.8
I.P. (eV)
N_2^+
304 Å

Fig. 18

Table 2. Branching Ratios for N_2^+

N_2^+ State	Branching ratios (%) 584Å	537Å	304Å
X $^2\Sigma_g^+$	37.7	29.2	11.6
A $^2\Pi_u$	54.6	60.3	20.6
B $^2\Sigma_u^+$	8.1	10.6	5.1
1 (D $^2\Pi_g$?)	-	-	12.1
2	-	-	8.6
3 $^2\Sigma_g^+$	-	-	42.1

lengths between 584 and 1216Å. A complete vibrational intensity analysis is given for all wavelengths studied. The outstanding result is the departure from the expected Franck-Condon distribution when absorption occurs in regions of autoionization. At 584Å absorption takes place directly into the ionization continuum and the vibrational intensities are in agreement with F.C. factors. The complete 584Å P.E. spectrum is shown in Fig. 19. In Fig. 20 the 584Å vibrational intensities of the ground state of the ion are compared with that caused by the Lyman gamma line at 972Å. The difference is striking, not only in the intensity distribution but in the number of vibrational lines observed. The reason for the difference is that the absorption process at 972Å proceeds mainly into highly excited states of NO.

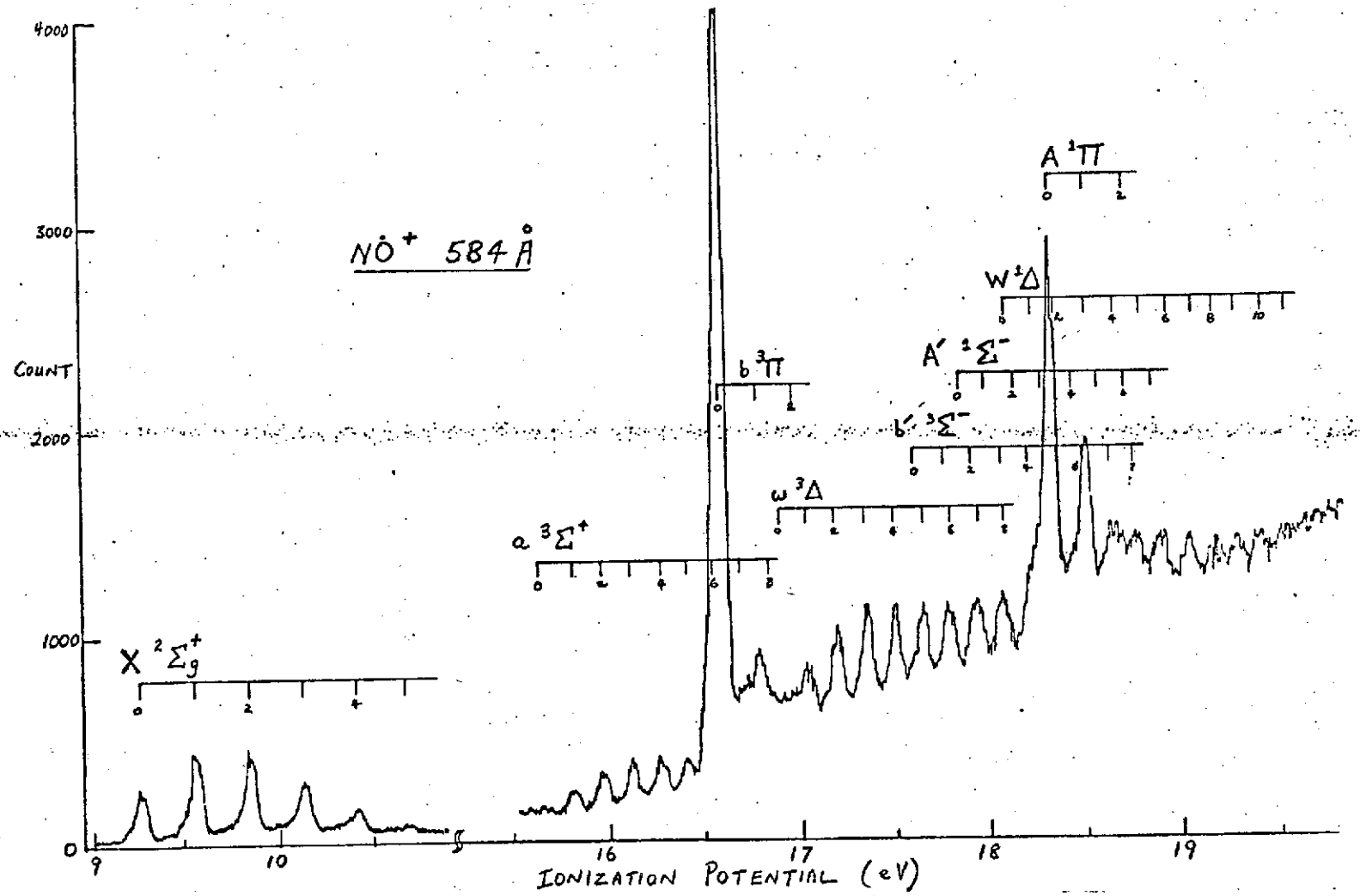
NO+ 584 Å
COUNT
4000
3000
2000
1000
0
X 2Σg+
a 3Σ+
b 3Π
ω 3Δ
A 1Π
W 1Δ
A' 1Σ−
b' 3Σ−
9
10
16
17
18
19
IONIZATION POTENTIAL (eV)

Fig. 19

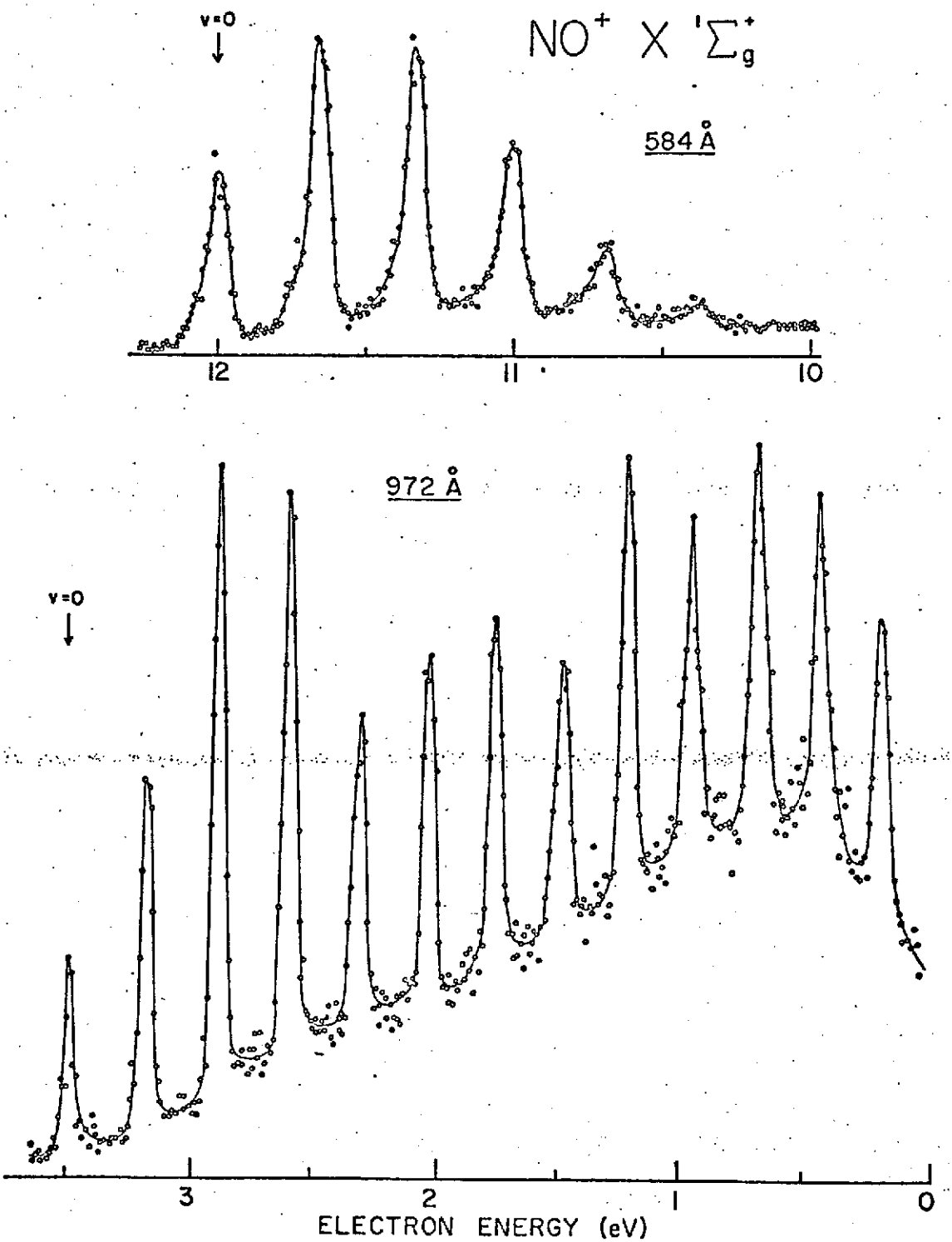

Fig. 20

These states subsequently auto-ionize into the continuum. Thus, the P.E. Spectra is controlled by the product of F.C. factors for transitions between the neutral ground state and the super-excited state with the F.C. factors for transitions from the super-excited state into the ionic state. Figure 21 shows the photoionization cross section of NO obtained by Watanabe. The lack of auto-ionizing structure from the ionization threshold to about 1150Å suggests that the vibrational intensities should be similar to the F.C. factors. Figure 22 verifies that this is so. However, for shorter wavelengths down to 950Å the photo-ionization cross sections are rich with auto-ionizing structure. The effect of this structure is shown dramatically in the vibrational intensities of the P.E. Spectra of lines between 972 and 1085Å (Figs. 23 and 24).

A comparison of the P.E. Spectra taken with the HI series Lyman α, β, γ are shown in Fig. 25. Only the Ly α line has a normal F.C. distribution of vibrational intensities. Table 3 lists the electronic branching ratios at 584Å.

Carbon Monoxide CO:

The P.E. Spectra of CO at 584Å is shown in Fig. 26 and the vibrational intensity analysis is given in Fig. 27.

The 304Å spectra is shown in Fig. 28. A new state is shown with an onset at 39 eV. Again it has a continuum structure indicating a dissociative ionization process is taking place with a considerable probability (41%). The branching

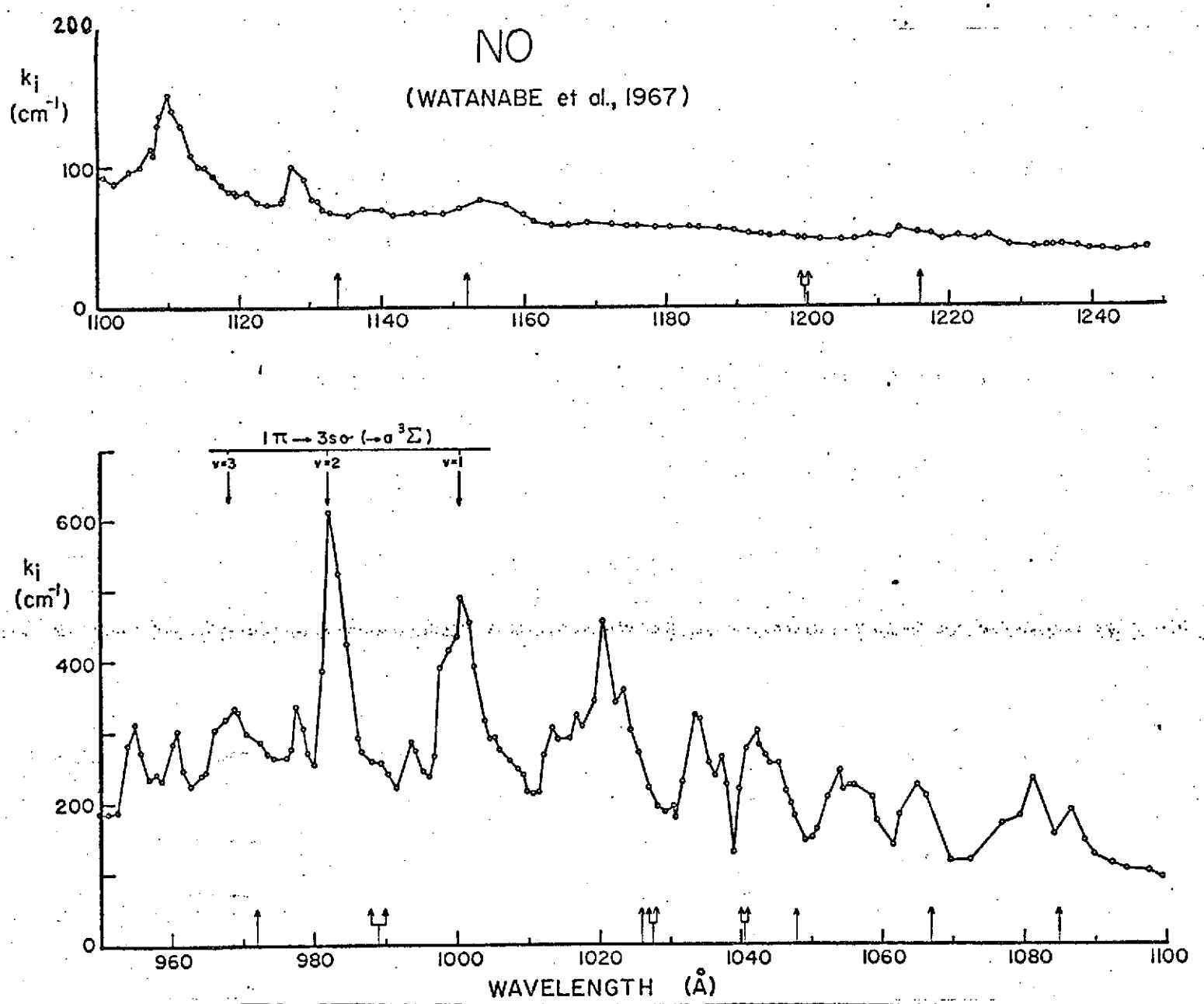
NO
(WATANABE et al., 1967)
k_j (cm^{-1})
200
100
0
1100
1120
1140
1160
1180
1200
1220
1240
$1\pi \rightarrow 3s\sigma$ ($\rightarrow a\,^3\Sigma$)
v=3
v=2
v=1
k_j (cm^{-1})
600
400
200
0
960
980
1000
1020
1040
1060
1080
1100
WAVELENGTH (Å)

Fig. 21

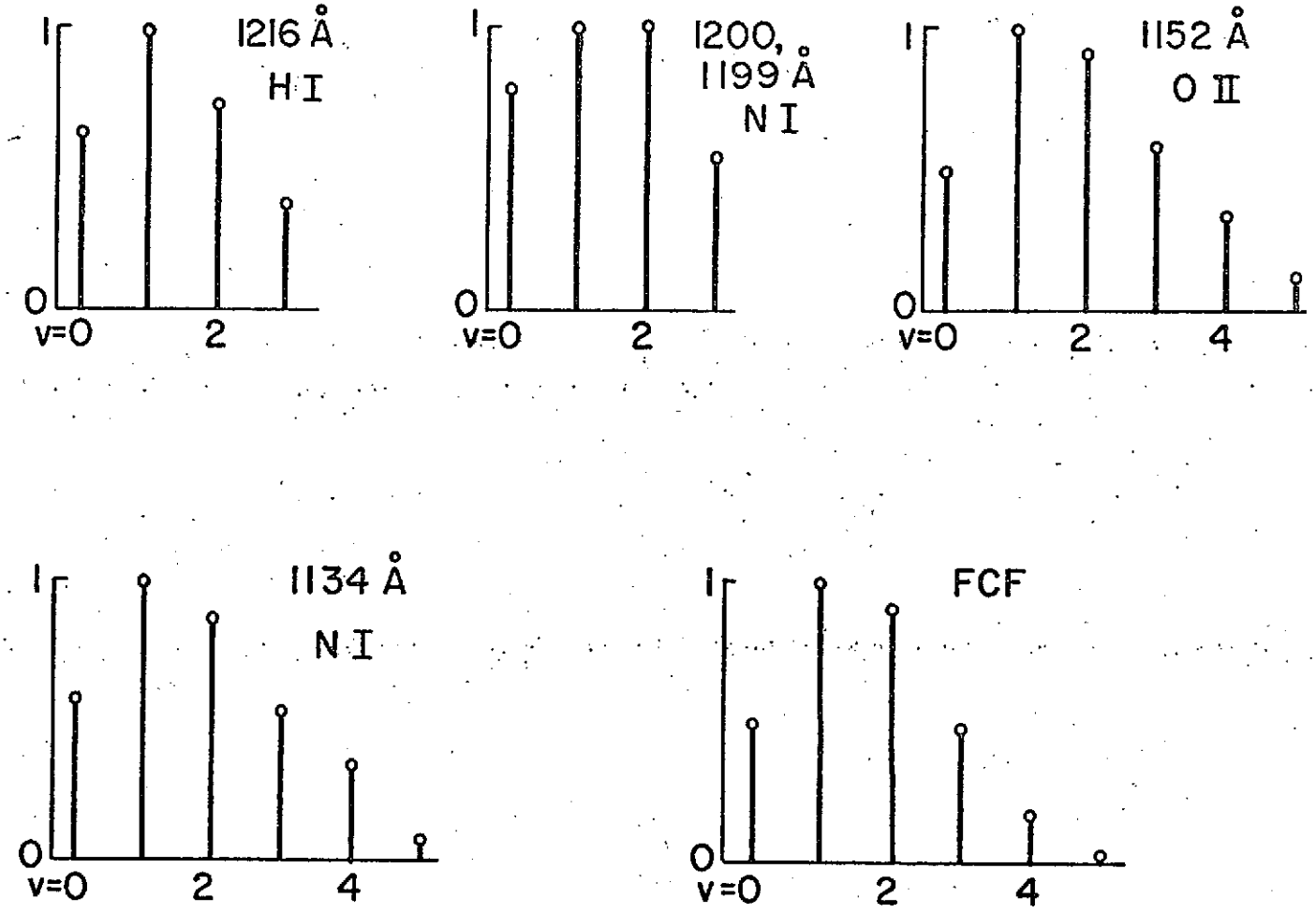
I
1216 Å
H I
0
v=0
2
I
1200,
1199 Å
N I
0
v=0
2
I
1152 Å
O II
0
v=0
2
4
I
1134 Å
N I
0
v=0
2
4
I
FCF
0
v=0
2
4

Fig. 22

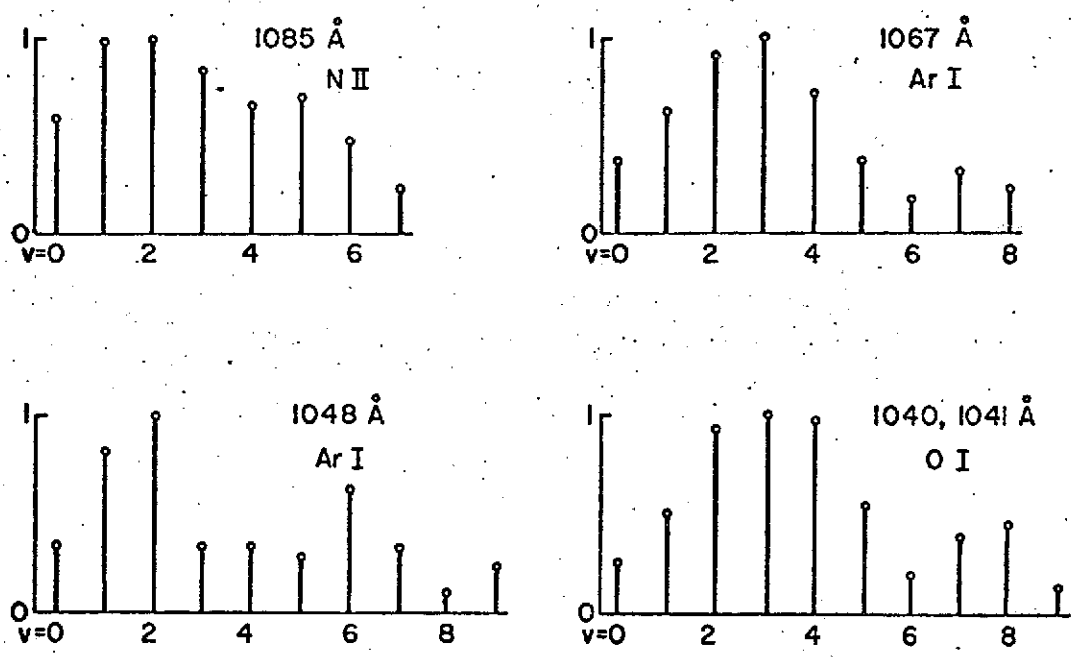
1085 Å
N II
I
0
v=0
2
4
6
1067 Å
Ar I
I
0
v=0
2
4
6
8
1048 Å
Ar I
I
0
v=0
2
4
6
8
1040, 1041 Å
O I
I
0
v=0
2
4
6
8

Fig. 23

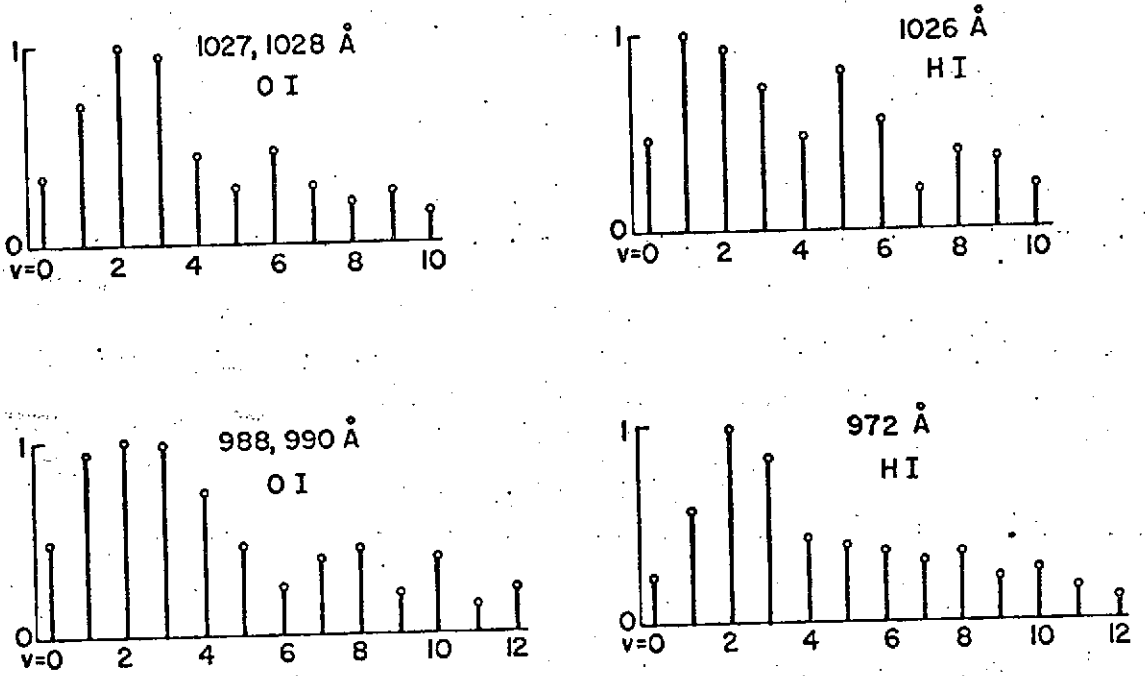
1027, 1028 Å
O I
I
0
v=0 2 4 6 8 10
1026 Å
H I
I
0
v=0 2 4 6 8 10
988, 990 Å
O I
I
0
v=0 2 4 6 8 10 12
972 Å
H I
I
0
v=0 2 4 6 8 10 12

Fig. 24

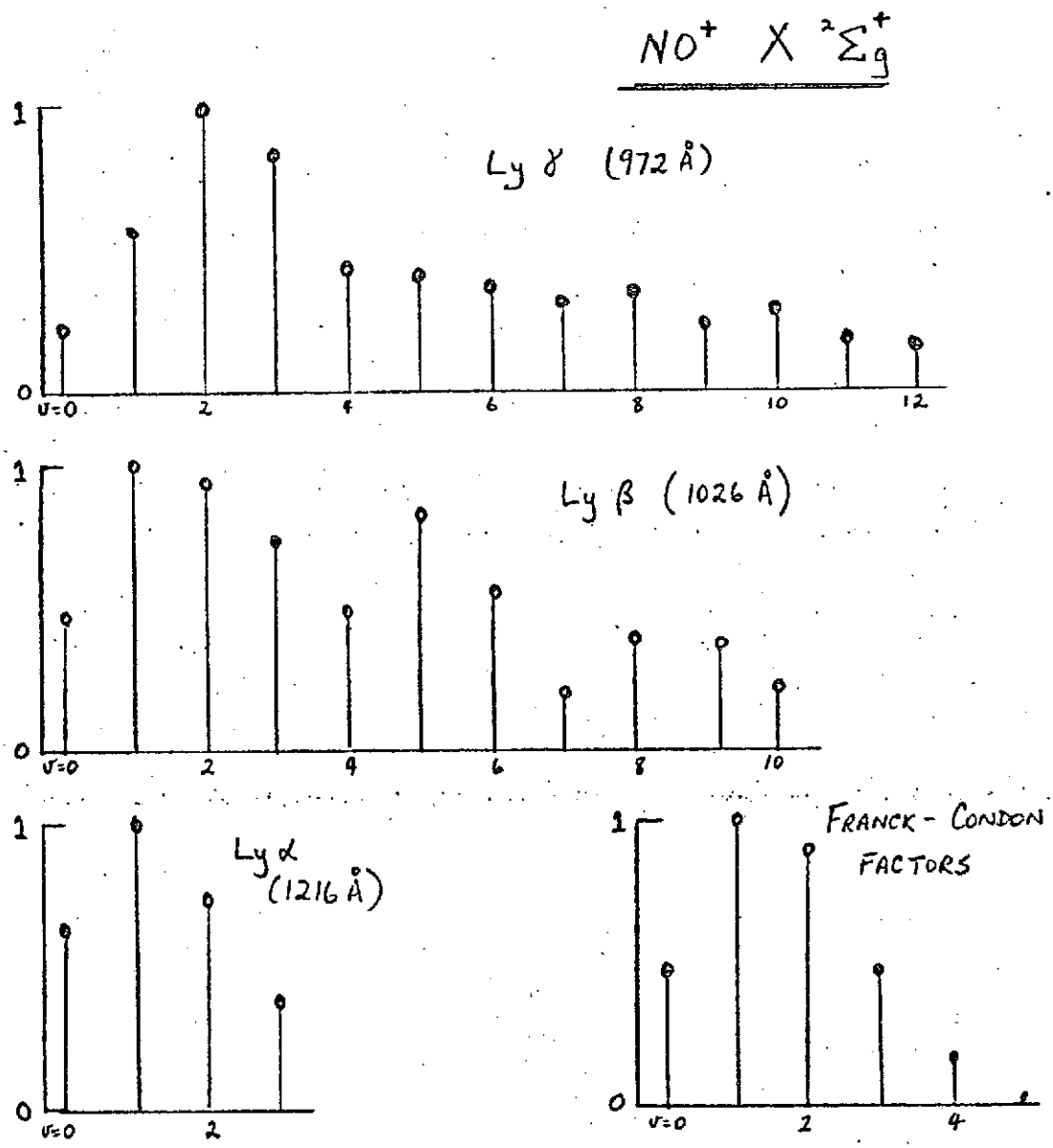
$NO^+ \; X \; {}^2\Sigma_g^+$
Ly γ (972 Å)
Ly β (1026 Å)
Ly α (1216 Å)
FRANCK - CONDON FACTORS
1
0
v=0
2
4
6
8
10
12

Fig. 25

Table 3. Branching Ratios for NO^+ at 584 Å

Ionic State	Branching Ratios (%)
$X\ ^1\Sigma^+$	12.1
$a\ ^3\Sigma^+$	6.6
$b\ ^3\Pi$	35.5
$\omega\ ^3\Delta$	11.6
$A\ ^1\Pi$	17.7
$b^1\ ^3\Sigma^-$, $A^1\ ^1\Sigma^-$, $W\ ^1\Delta$	5.9
$c\ ^3\Pi$	<0.4

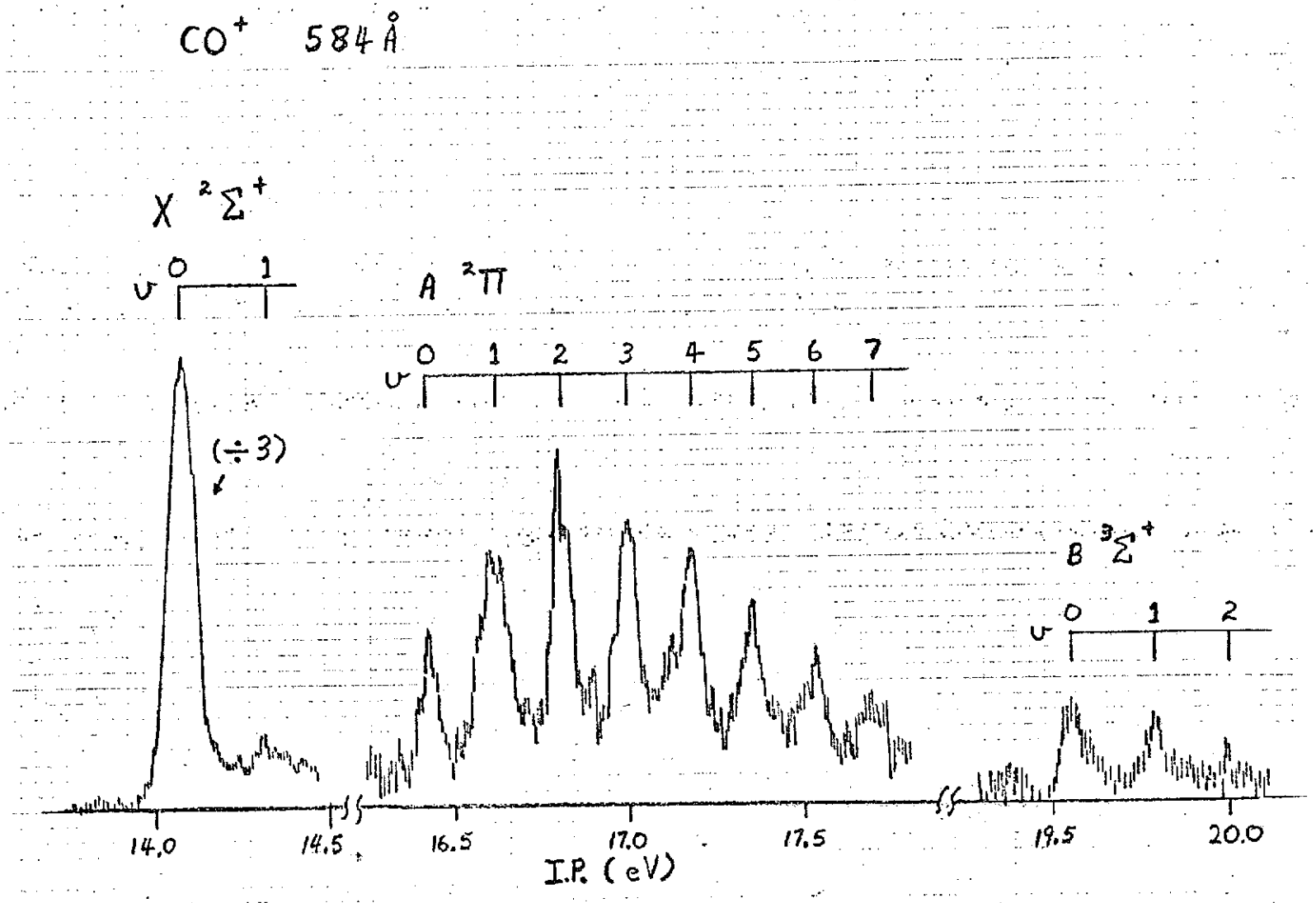
CO+ 584 Å
X 2Σ+
υ 0 1
A 2Π
0 1 2 3 4 5 6 7
(÷3)
B 3Σ+
0 1 2
14.0
14.5
16.5
17.0
17.5
19.5
20.0
I.P. (eV)

Fig. 26

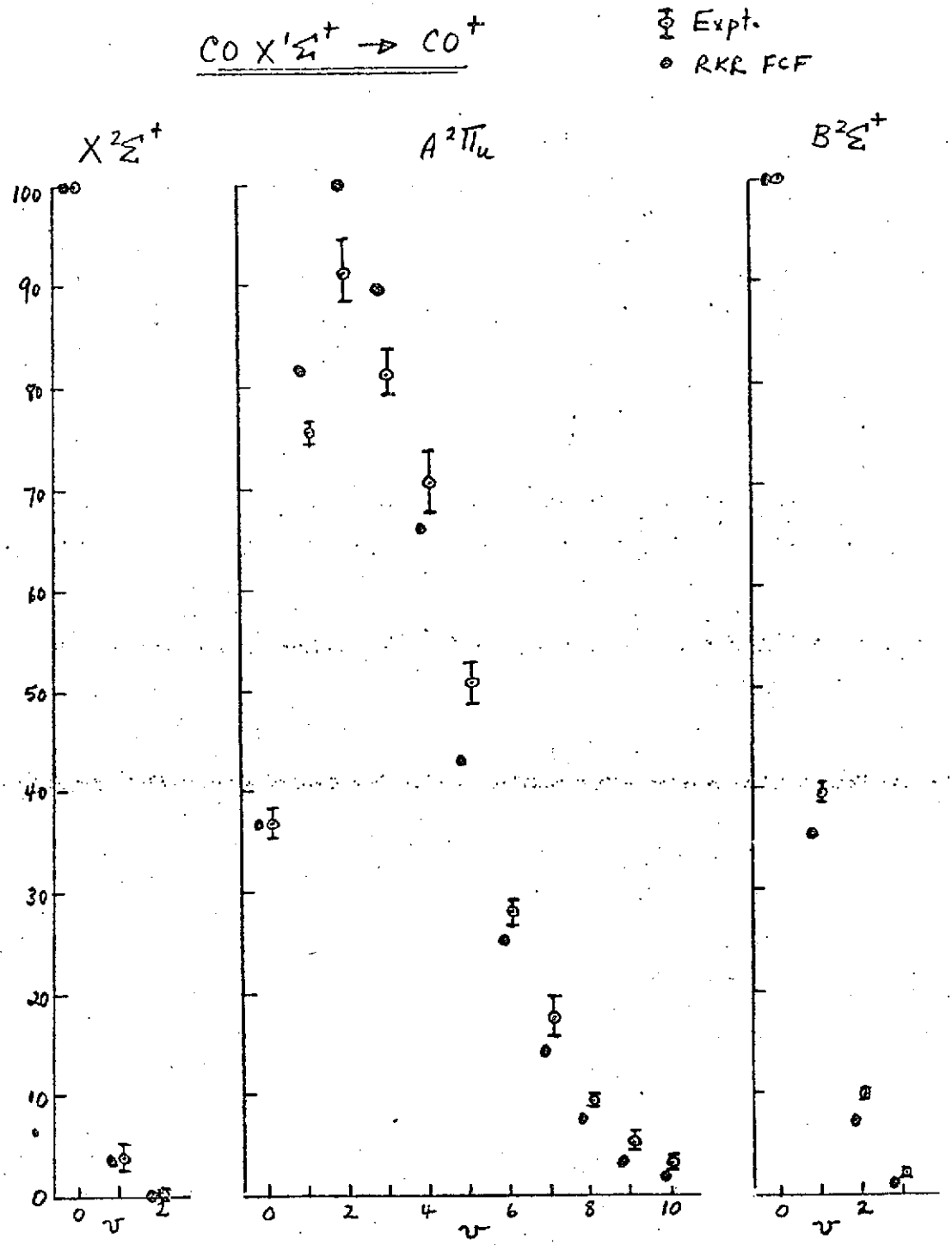
CO X $^1\Sigma^+$ → CO$^+$
Expt.
RKR FCF
X $^2\Sigma^+$
A $^2\Pi_u$
B $^2\Sigma^+$
100
90
80
70
60
50
40
30
20
10
0
0
2
0
2
4
6
8
10
0
2
v
v
v

Fig. 27

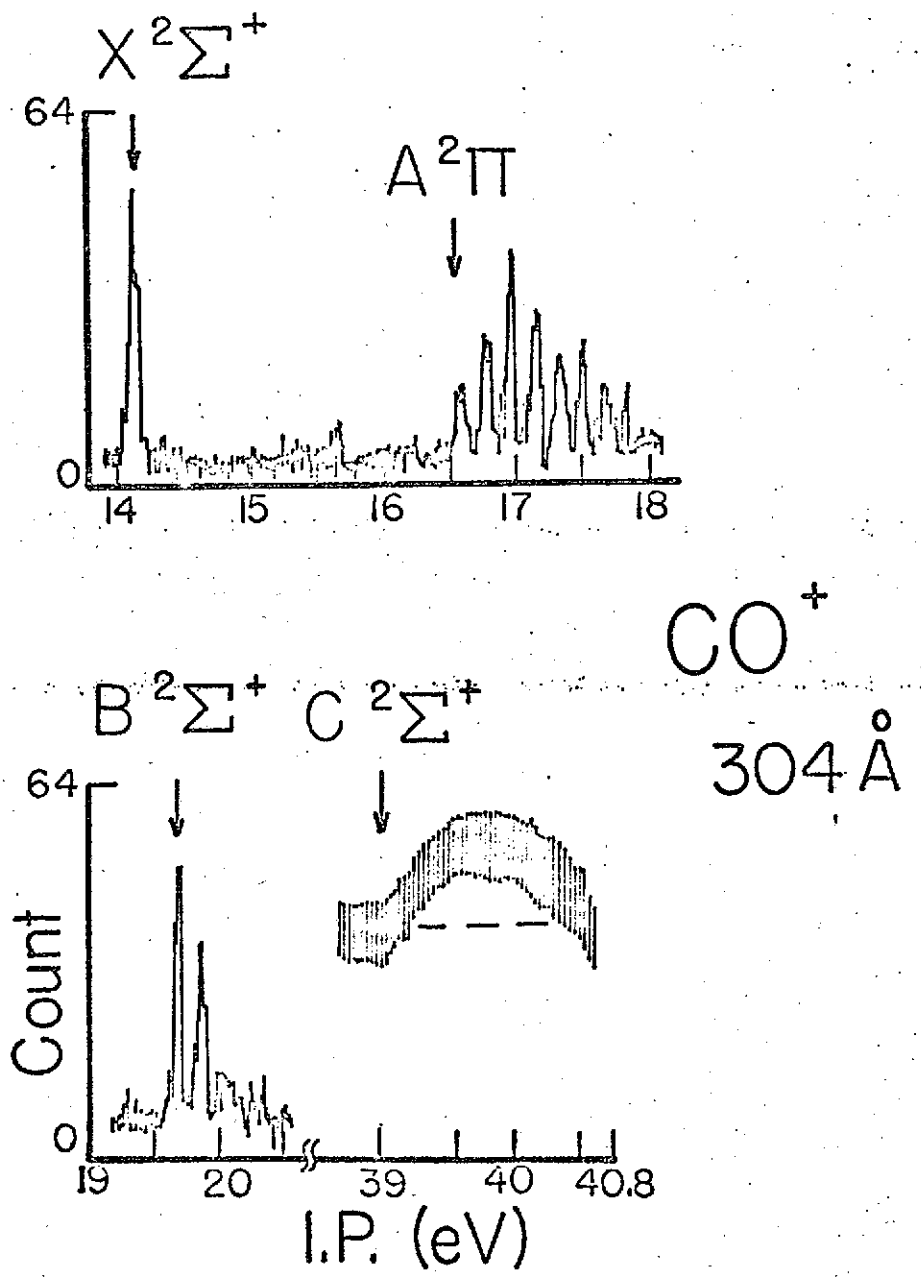
X ²Σ⁺
64
0
A ²Π
14
15
16
17
18
CO⁺
304 Å
B ²Σ⁺
C ²Σ⁺
64
Count
0
19
20
39
40
40.8
I.P. (eV)

Fig. 28

Table 4. Branching Ratios for CO^+

CO^+ State	Branching ratios (%) 584 Å	537 Å	304 Å
$X\ ^2\Sigma^+$	25.3	29.3	9.1
$A\ ^2\Pi$	62.3	57.8	32.0
$B\ ^2\Sigma^+$	12.6	12.9	17.6
$C\ ^2\Sigma^+$	-	-	41.2

ratios are listed in Table 4 for the 584, 537, and 304Å lines.

Carbon Dioxide CO_2:

Carbon dioxide has been the subject of three published papers originating from this work and will not be elaborated upon. However, the 304Å P.E. Spectra is reproduced here in Fig. 29 to complete the series. Again new states appear around 37 eV and constitute about 62% of the ionization process. Dissociative ionization is indicated by the structure of the P.E. peak. The electronic branching ratios are shown in Table 5 for 584, 537, and 304Å.

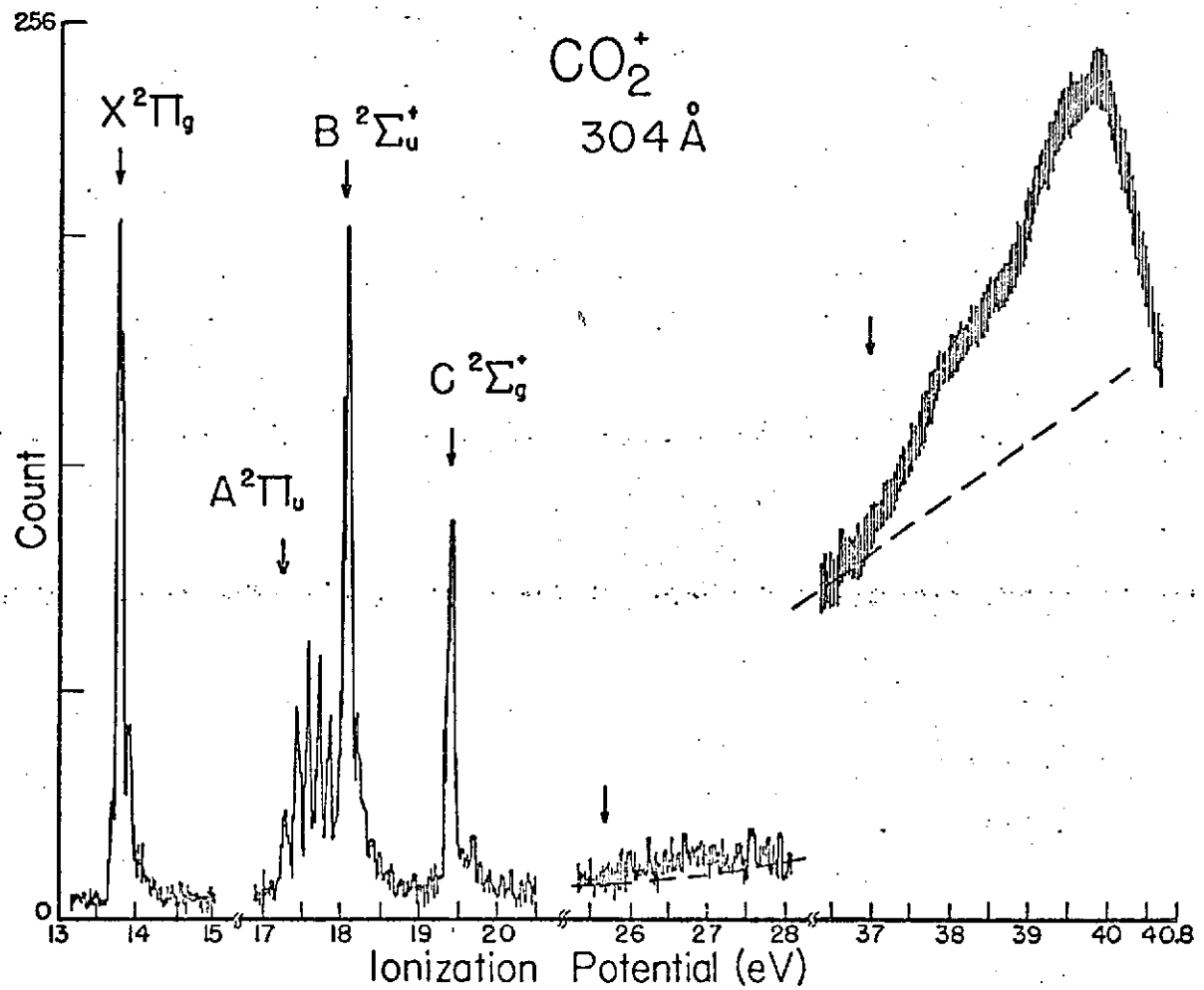
256
Count
0
CO_2^+
304 Å
$X^2\Pi_g$
$B^2\Sigma_u^+$
$C^2\Sigma_g^+$
$A^2\Pi_u$
13
14
15
17
18
19
20
26
27
28
37
38
39
40
40.8
Ionization Potential (eV)

Fig. 29

Table 5. Branching Ratios for CO_2^+

CO_2^+ State	Branching Ratios (%) 584Å	537Å	304Å
X $^2\Pi_g$	22.6	26.6	9.5
A $^2\Pi_u$	29.1	27.8	10.5
B $^2\Sigma_u^+$	44.8	37.8	10.4
C $^2\Sigma_g$	4.3	7.8	6.0
a	-	-	2.2
$^2\Sigma_u + {}^2\Sigma_g$	-	-	61.5

Fluorescent Measurements

The fluorescence of CO_2 under photon bombardment has been measured from threshold to 185Å. Absolute cross sections for fluorescence have been reported in the literature. Figure 30 illustrates the fluorescent yield of CO_2 from 700 to 185Å. Apparatus is currently being constructed to survey the nature of the short wavelength fluorescent radiation observed. This work is continuing and will be extended to observations of 304Å fluorescence from He.

Some Preliminary Results

A P.E. Spectrum of O_2 excited by a microwave power unit was attempted using the spherical grid retarding potential analyzer. However, with the number of species present, namely, O, O_2, $O_2(^1\Delta)$, O_2^+, etc. it was clear that an integral spectrum was of no use. Consequently, a high resolution differential analyzer such as the mirror type is under construction to continue this line of research.

The current program has developed a strong capability in our laboratory to pursue photoelectron and fluorescence studies. The present work is being continued and expanded upon.

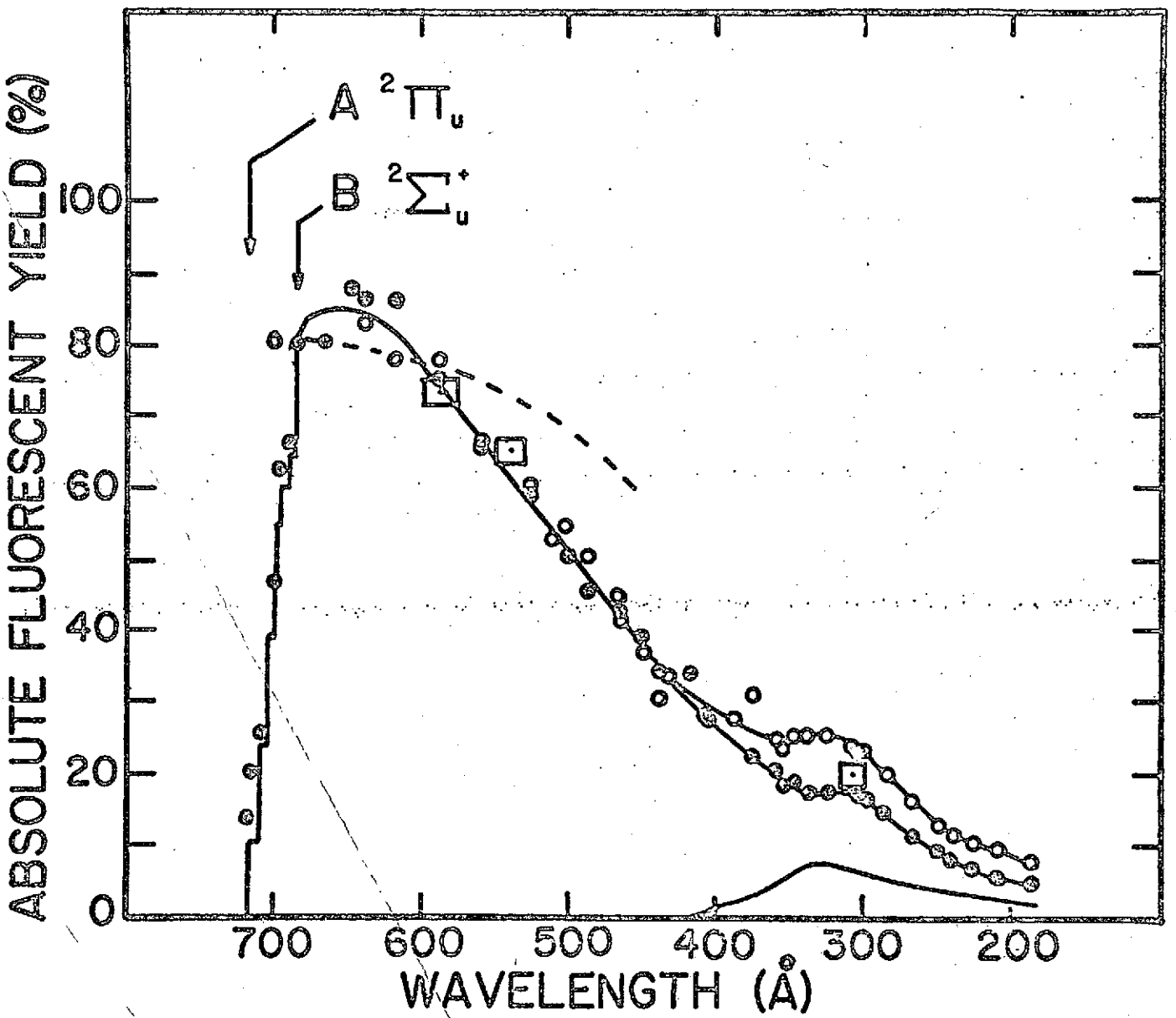
ABSOLUTE FLUORESCENT YIELD (%)
0
20
40
60
80
100
A $^2\Pi_u$
B $^2\Sigma_u^+$
700
600
500
400
300
200
WAVELENGTH (Å)

Fig. 30.